Science Advances
AAAS

# Supplementary Materials for

## Type 1 immunity enables neonatal thymic ILC1 production

Peter Tougaard *et al.*

Corresponding author: Peter Tougaard, peter.tougaard@irc.vib-ugent.be;
Peter Vandenabeele, peter.vandenabeele@irc.vib-ugent.be

*Sci. Adv.* **10**, eadh5520 (2024)
DOI: 10.1126/sciadv.adh5520

**The PDF file includes:**

Supplementary Materials and Methods
Figs. S1 to S7
Tables S1 to S28
Legend for movie S1
Legend for data file S1
References

**Other Supplementary Material for this manuscript includes the following:**

Movie S1
Data file S1

**Supplementary Materials**

## Supplementary Materials and Methods

### Methods S1: *Single-cell RNA seq and CITE-seq (extended protocol and quality control)*

Size selection with SPRIselect Reagent Kit (Beckman Coulter, B23318) was applied to separate the amplified cDNA molecules for 3' gene expression and cell surface protein construction. TotalSeq-A protein library construction including sample index PCR using Illumina's Truseq Small RNA primer sets and SPRIselect size selection was performed according to the manufacturer's instructions. The cDNA content of pre-fragmentation and post-sample index PCR samples was analyzed using 2100 BioAnalyzer (Agilent). Sequencing libraries were loaded on a HiSeq4000 flow cell (NTOC) and an Illumina NovaSeq flow cell (tissue) at VIB Nucleomics core with sequencing settings according to the recommendations of 10x Genomics, pooled in a 90:10 ratio for the combined 3′ gene expression and cell surface protein samples respectively. The Cell Ranger pipeline (10x Genomics, version 3.1.0) was used to perform sample demultiplexing and to generate FASTQ files for read 1, read 2 and the i7 sample index for the gene expression and cell surface protein libraries. Read 2 of the gene expression libraries was mapped to the mouse reference genome (GRCm38.99). Subsequent barcode processing, unique molecular identifiers filtering and gene counting were performed using the Cell Ranger suite. CITE-seq reads were quantified using the feature-barcoding functionality. The average mean reads per cell across the NTOC libraries and tissue libraries were 13268 and 28039, respectively, with an average sequencing saturation of 22.9% and 51.76%, respectively, calculated by Cell Ranger (version 3.1.0). In total 4 NTOC libraries and 8 tissue libraries were created in this study, entailing 61501 and 88947 cells, respectively.

### Methods S2: *scRNA-seq and CITE-seq processing and analysis*

The aggregation of NTOC samples was done using the Cell Ranger Aggr software from 10x Genomics. Pre-processing of the data was done by the SCRAN and Scater R packages *(56)*. Outlier cells were identified based on three metrics (library size, number of expressed genes and mitochondrial proportion), and cells were tagged as outliers when they were a median absolute deviation (MAD) away from the median value of each metric across all cells. The outliers were determined with a setting of three MADs for library size and the number of expressed genes and four MADs for mitochondrial proportion. The low-quality cells (low/high UMI counts, low/high number of genes, high % mitochondrial genes) were removed from the analysis. Genes expressed in less than 3 cells and cells expressing less than 200 genes were removed. The raw counts were processed with the Seurat R package (v 3.2.3) *(57)* using the following functions with default parameters unless stated otherwise: NormalizeData, FindVariableFeatures, ScaleData, RunPCA, FindNeighbors, FindClusters (resolution: 0.8), RunUMAP (dims = 1:25). The tissue libraries were merged and processed with the Seurat package (v 4.1.1) using the following functions with default parameters unless stated otherwise: NormalizeData, FindVariableFeatues, ScaleData, RunPCA, FindNeighbors (dims = 1:30), FindClusters (resolution: 0.3), RunUMAP (dims = 1:30). Subsets were made of both datasets (NTOC dataset was filtered on ILC1s, γδT17 cells and CD4 T cells; tissue dataset was filtered on $Ncr1^{+}CD3e^{-}$ cells). These subsets were integrated and batch corrected with the Harmony package (v 0.1.0) *(57)* using the following pipeline: NormalizeData, FindVariableFeatues, ScaleData, RunPCA (npcs = 150), RunHarmony, FindNeighbors (dims = 1:50), FindClusters (resolution: 1.8), RunUMAP (dims = 1:50). Clusters were further manually curated. Figures were made using the VlnPlot, DimPlot, FeaturePlot and DotPlot functions of the Seurat package.

**References:** *(56)* and *(57)* only appear in Supplementary Materials and Methods

# Supplementary Figures

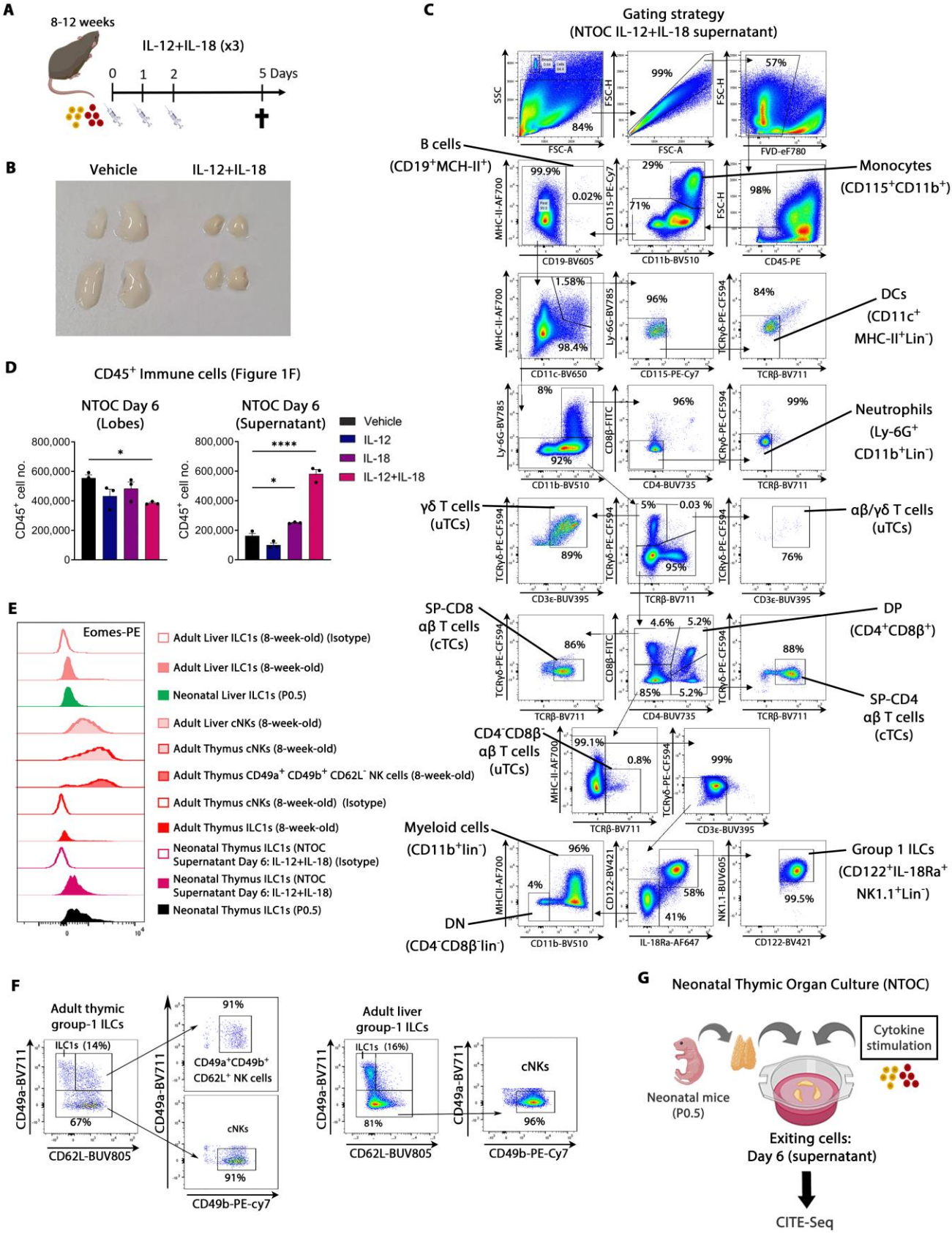


**Fig. S1: Type-1 inflammation induces expansion of thymic-exiting ILC1s during NTOC.**

**(A)** Schematic of cytokine injection model where adult mice are injected three times with IL12+IL-18. **(B)** As shown in (A), a picture of both thymic lobes from two 8-week-old mice 5 days after the first injection with IL-12+IL-18 or Vehicle and representative of at least three independent experiments. **(C)** Representative flow cytometry gating strategy for Fig. 1F. **(D)** Total CD45$^+$ cells in vehicle control conditions and cytokine stimulatory conditions in lobes and supernatant from neonatal thymic organ culture (NTOC) in Fig. 1F. **(E)** Intracellular Eomes expression shown as representative histograms on ILC1s (CD122$^+$NK1.1$^+$CD49a$^+$CD62L$^-$Lin$^-$) and cNK cells (CD122$^+$NK1.1$^+$CD49b$^+$CD49a$^-$Lin$^-$) from the liver and thymus (adults and neonates), and IL-12+IL-18 NTOC supernatant with corresponding isotype controls (open histograms), as well as unconventional adult thymic NK (CD122$^+$NK1.1$^+$CD49a$^+$CD49b$^+$CD62L$^+$Lin$^-$), gating shown in (F) and representative of $n$ = 5-6 biological replicates from two independent experiments. **(F)** Representative gating strategy from CD122$^+$NK1.1$^+$Lin$^-$ gate used for differentiation of adult and neonatal ILC1s, cNK cells, and unconventional adult thymic NK cells in (E). **(G)** Schematic of NTOC setup for CITE-seq analysis of supernatant cells. **Statistics:** (D) One-way Anova * p < 0.05, ****p < 0.0001. Lin$^-$, Lineage negative, defined as TCRβ$^-$TCRγδ$^-$CD3ε$^-$CD4$^-$CD8β$^-$Ter-119$^-$Ly-6G$^-$CD19$^-$CD11c$^-$F4/80$^-$. cTC, Conventional T cells; uTC, Unconventional T cells; DC, Dendritic cell; DN, Double negative (CD4 and CD8 negative thymocytes); DP, Double positive (CD4 and CD8 positive thymocytes).

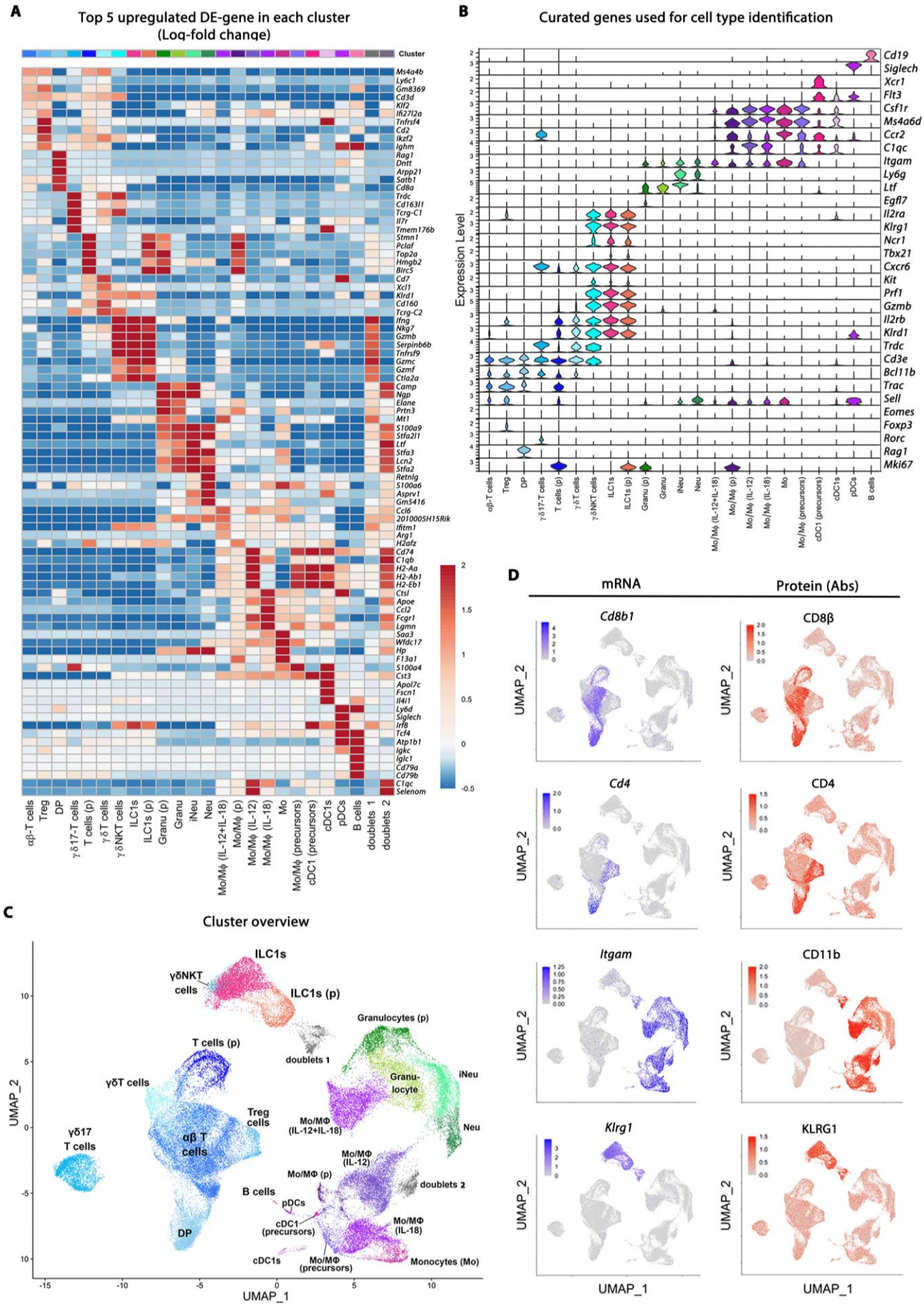


**Fig. S2: scRNAseq analysis of thymus-exiting ILC1s during NTOC.**

**(A)** Heatmap showing top-5 upregulated Differentially expressed gene (DE)-genes for each of the 23 scRNAseq clusters and doublets from neonatal thymic organ culture (NTOC). **(B)** Violin plot of 23 scRNAseq clusters showing genes used for cell type and cell state identification (proliferation marker: *Mki67*). **(C)** Uniform Manifold Approximation and Projection **(**UMAP) plot of scRNAseq data, dividing the cells into 23 clusters and two clusters of doublets. **(D)** UMAP feature plots of CITE-seq data showing gene expression (mRNA) and corresponding surface protein (Abs) based on CITE-seq antibodies. (p), proliferating; Treg, Regulator T cell; DP, Double positive; Granu, Granunolcytes; iNeu, immature neutrophils; Neu, Neutrophils; Mo/MΦ, Monocytes/Macrophages; cDC1, conventional type 1 DCs; pDC, plasmacytoid DCs.

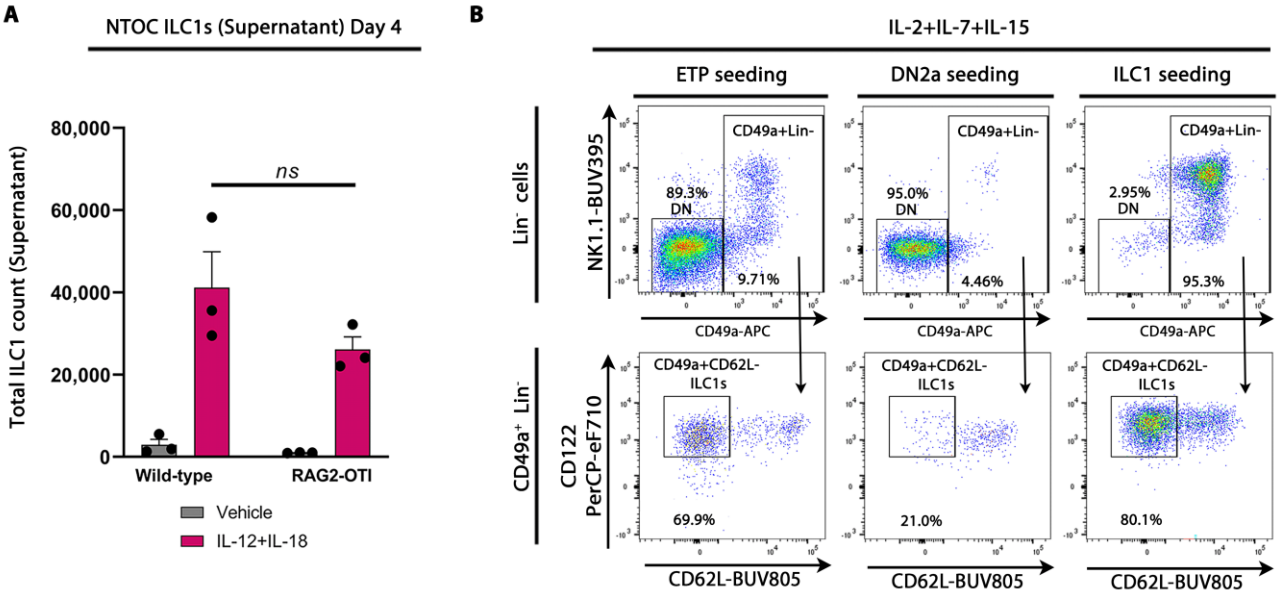


**Fig. S3: IL-12+IL-18-induced thymic ILC1s are RAG independent.**

**(A)** Bar plot showing ILC1s exiting neonatal thymic organ culture (NTOC) lobes into the supernatant after 4 days of culture with *two lobes* per condition. Thymic lobes derived from either wild-type or *Rag2*$^{-/-}$ OTI TCR transgene mice. Pooled from two independent experiments with $n = 3$ biological replicates. Error bars display means ± SEM. **(B)** Flow plots showing ILC1s (CD122$^{+}$CD49a$^{+}$CD62L$^{-}$lin$^{-}$) developing and expanding from (ETPs and ILC1) seeded cells following 6 days of OP9-DL1 co-culture for ETPs (CD117$^{(hi)}$CD44$^{+}$CD25$^{-}$CD122$^{-}$Lin$^{-}$), DN2a (CD117$^{(hi)}$CD44$^{+}$CD25$^{+}$CD122$^{-}$Lin$^{-}$), or ILC1s (CD122$^{+}$Lin$^{-}$) from the neonatal thymus. **Statistics**: Two-way ANOVA, *ns* = not significant. DN, Double negative; ETP, Early Thymic Progenitors; Lin$^{-}$, Lineage negative, defined as TCRβ$^{-}$TCRγδ$^{-}$CD3e$^{-}$CD4$^{-}$CD8β$^{-}$Ly-6G$^{-}$F4/80$^{-}$CD19$^{-}$CD11c$^{-}$.

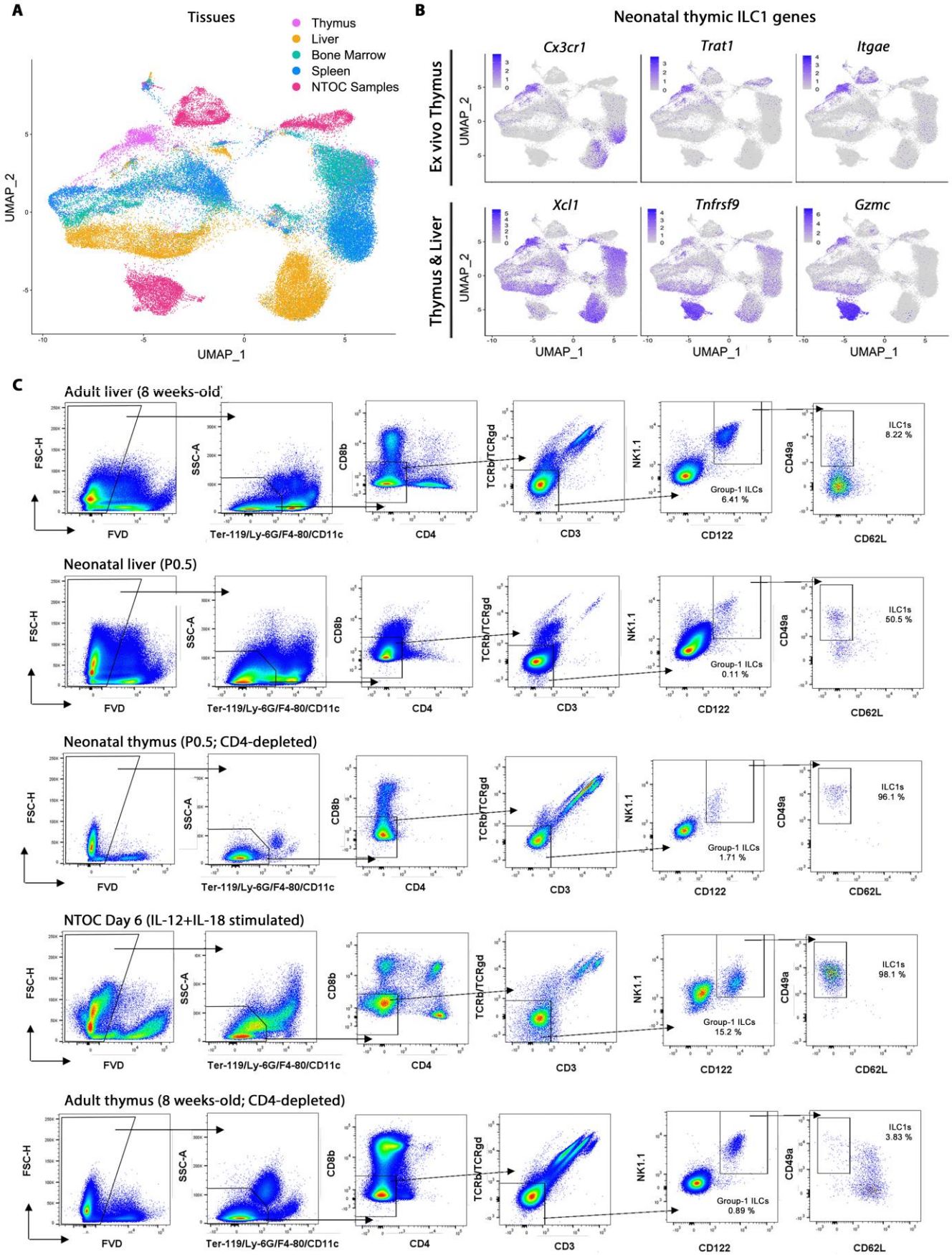


**Fig. S4: Neonatal thymic ILC1s display high expression of *Cx3cr1*, *Trat1*, and *Itgae*.**

**(A)** Uniform Manifold Approximation and Projection **(**UMAP) of Harmony integrated data from (Fig. 4A**)**, showing an overview of the different tissues illustrated in (Fig. 4C; showing the neonatal and adult tissues with the same color). **(B)** UMAP feature plots of prominent curated differentially expressed genes (DE)-genes from neonatal thymus ILC1s. **(C)** Representative gating strategy for histograms in (Fig. 4F) on $CD122^{+}NK1.1^{+}CD49a^{+}CD62L^{-}Lin^{-}$ ILC1s. Same gating strategy was used for histograms in (Fig. 1G) until group-1 ILCs ($CD122^{+}NK1.1^{+}Lin^{-}$) to show ILC1 and cNK markers.

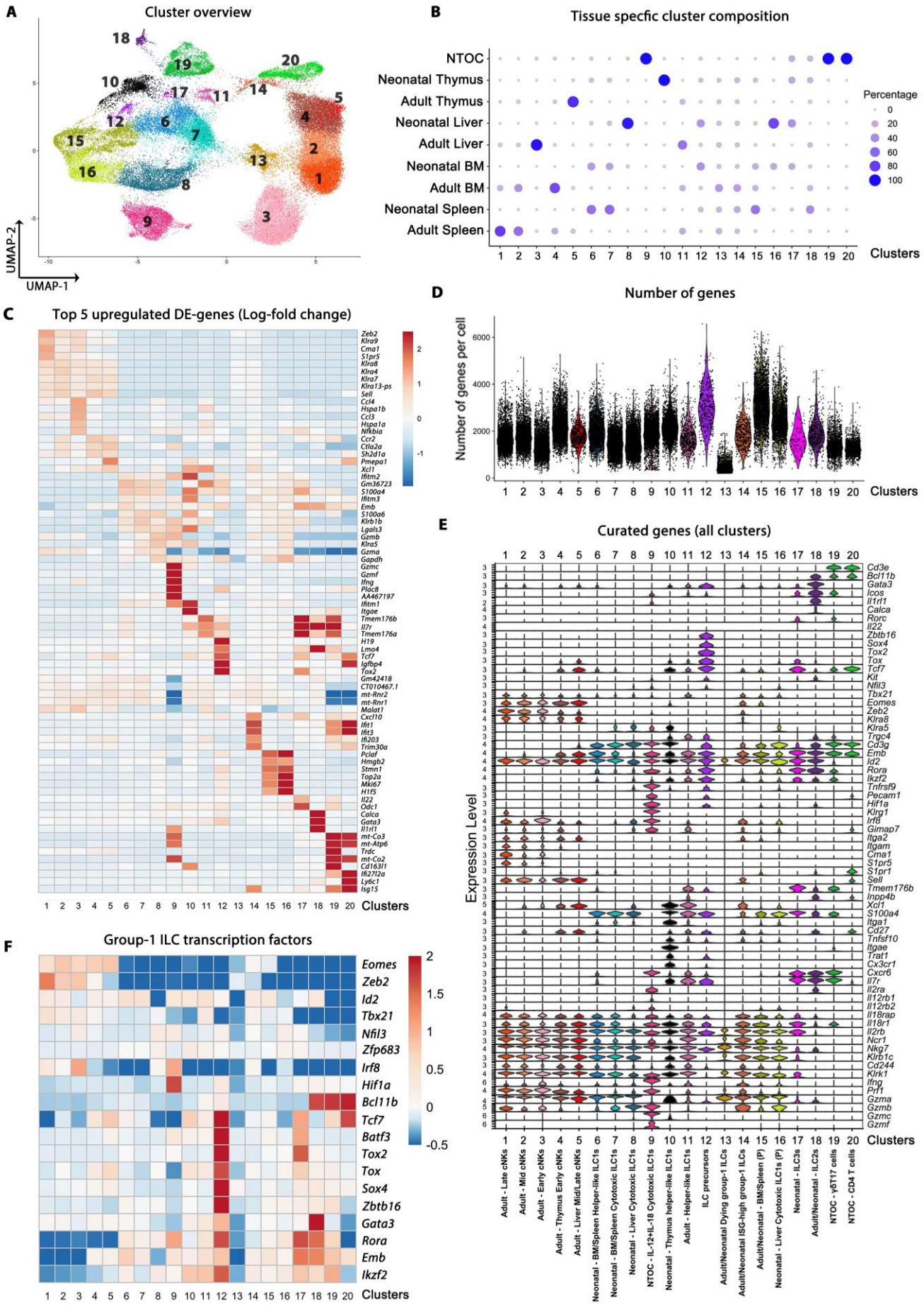


**Fig. S5: Steady-state neonatal thymic ILC1s display a unique and immature phenotype.**

**(A)** Uniform Manifold Approximation and Projection (UMAP) overview of all 20 clusters in Harmony-integrated scRNAseq comparison of group-1 ILCs in 8-weeks-old adult and P0.5 neonatal mice across tissues (Thymus, Liver, Spleen, Bone marrow) and NTOC clusters. **(B)** Cluster composition overview, showing the tissue distribution of each of the 20 clusters. **(C)** Top-5 upregulated differentially expressed genes (DE)-genes in all clusters. **(D)** Number of genes per cell for each cluster. **(E)** Violin plot of gene expression in all 20 clusters with an extended list of curated genes visualizing markers for cell type, maturation, and function. **(F)** Heatmap of group-1 ILC transcription factors in all clusters.

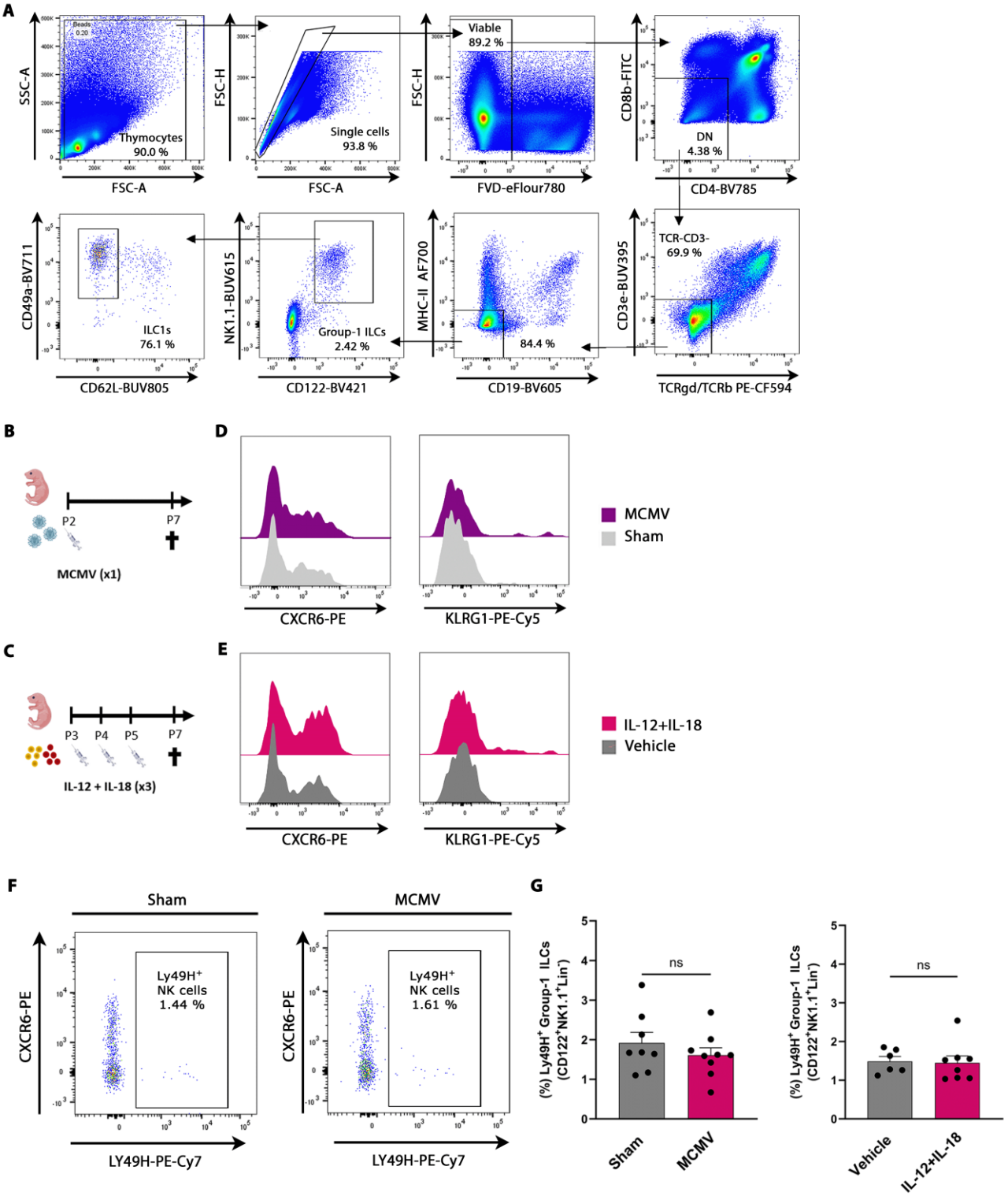


**Fig. S6: Thymic ILC1s display enhanced CXCR6 and KLRG1 expression during MCMV infection.**

**(A)** Gating strategy for thymic ILC1s in Fig. 6E to 6J. **(B)** Schematic of mice infected with murine cytomegalovirus (MCMV) or sham for 5 days and terminated on P7. **(C)** Schematic of mice injected three times from P3 to P5 with IL-12+IL-18 or Vehicle and terminated on P7. **(D)** Representative histograms of ILC1s expressing CXCR6 and KLRG1 in MCMV and sham infected neonates. **(E)** Representative histograms of ILC1s expressing CXCR6 and KLRG1 in IL-12+IL-18 injected and Vehicle-injected neonates. **(F)** Gating strategy of Ly49H$^+$ cells in the thymic group-1 ILC (CD122$^+$NK1.1$^+$Lin$^-$) compartment in MCMV and Sham-infected neonates. **(G)** Ly49H$^+$ cells in the thymic group-1 ILC (CD122$^+$NK1.1$^+$Lin$^-$) as shown in (F) for MCMV and Sham-infected neonates (Left) and IL-12+IL-18 injected and Vehicle-injected neonates (Right). Data are shown for n = 8-9 (MCMV) and n = 7-9 (IL-12+IL-18) neonates and representative of two independent experiments.

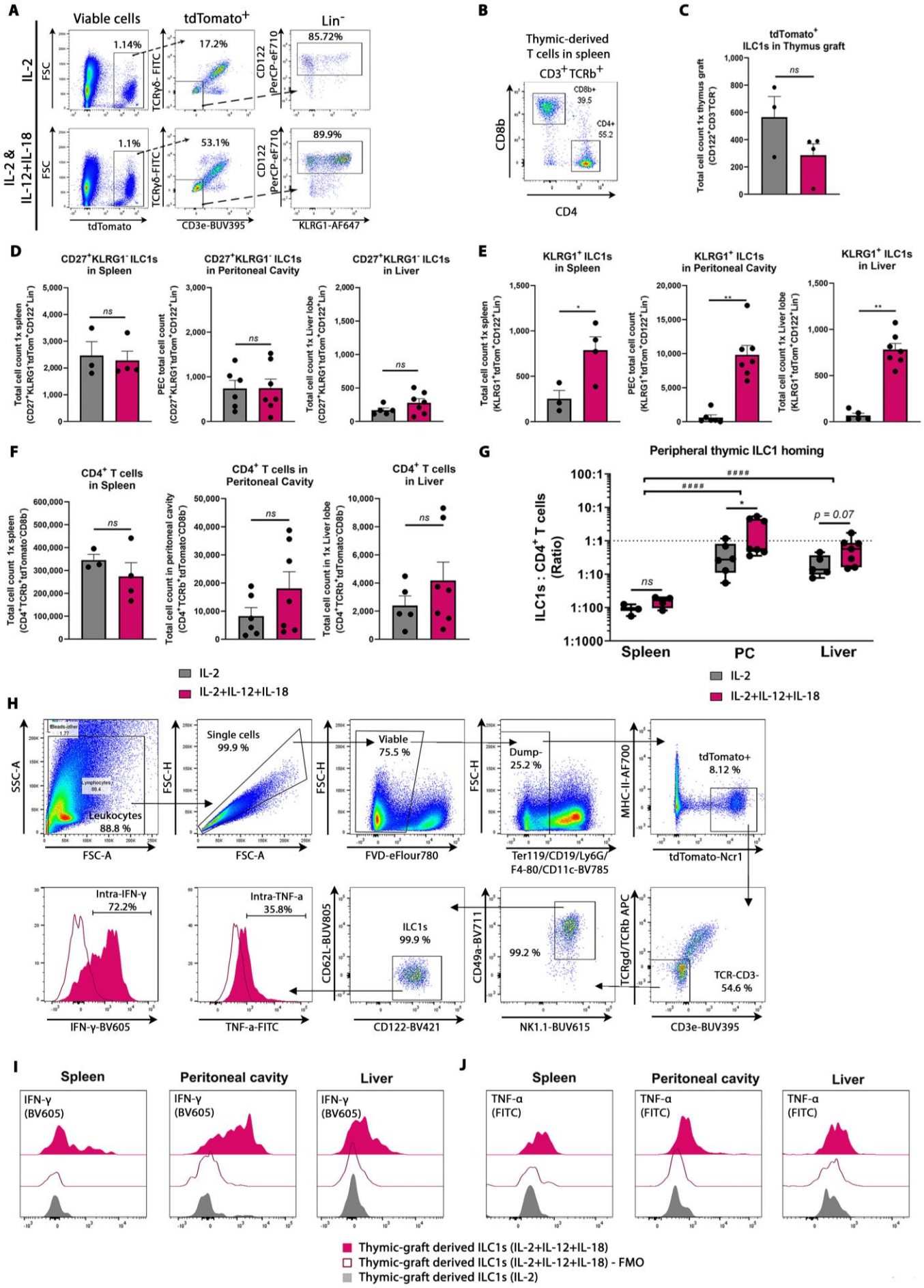


**Fig. S7: KLRG1$^+$ thymic ILC1s home to the liver and the peritoneal cavity.**

**(A)** Representative gating strategy showing important gating steps for gating tdTomato$^+$ ILC1s in IL-2 injected vs IL-2+IL-12+IL-18 injected cells from the peritoneal cavity shown in Fig. 7C, additional gating shown in Fig. 7D. **(B)** Flow plot showing splenic reconstitutions of CD4 and CD8 T cells in IL-2 injected mice 6 days after

grafting representative of five biological replicates, gating on viable $CD3^+TCRb^+$ cells. **(C)** Bar plot of ILC1s in the thymus graft from *n* = 3 mice per condition and are representative of three independent experiments. **(D)** Bar plots of thymus graft-derived $CD27^+KLRG1^-$ ILC1s in the spleen, peritoneal cavity, and liver. **(E)** Bar plots of thymus graft-derived $KLRG1^+$ ILC1s in the spleen, peritoneal cavity, and liver. **(F)** Bar plots of thymus graft-derived CD4 T cells in the spleen, peritoneal cavity and liver. Data are combined from two independent experiments. **(G)** Box plots showing the count *ratio* on a Log10-scale between thymus-graft-derived ILC1s : CD4 T cells in the spleen, peritoneal cavity (PC), and liver. (C, D, and F) Data are pooled from two independent experiments from *n* = 3-4 (Spleen), *n* = 6-7 (PC), and *n* = 5-7 (Liver) mice per condition and representative of four independent experiments. (C-G) Each dot represents a separate thymus grafted mouse and pooled from two independent experiments and representing four independent experiments. **(H)** Representative gating strategy for $tdTomato^+$ ILC1s in intracellular cytokine experiment shown from the peritoneal cavity in Fig. 7F. **(I and J)** Intracellular cytokine expression of (I) IFN-γ and (J) TNF-α in thymic graft-derived ILC1s from indicated organs. Expression is shown as histograms after 4 hours after Brefeldin A & Monensin block and no further stimulation and are representative of *n* = 6 mice per condition from two independent experiments. **Statistics**; (C-F) Unpaired T test (two-tailed), and (G); Two-way ANOVA between treatments: **** $p < 0.0001$, *ns* = Not significant. (G) Two-way anova between tissues: $^{\#\#\#\#}$ $p < 0.0001$. Lin-, Lineage negative, defined as: $TCR\beta^-TCR\gamma\delta^-CD3e^-CD4^-CD8\beta^-Ter\text{-}119^-Ly\text{-}6G^-$; PC, Peritoneal cavity.

**Supplementary Tables**

**Table S1: Flow cytometry, cell sorting and imaging antibodies**

| *Antigen* | *Fluorochrome* | *Clone* | *Source* | *Cat#* | *Dilution (1:X)* | *Notes* |
|---|---|---|---|---|---|---|
| **CD49b** | FITC | DX5 | ThermoFisher | 11-5971 | 1/200 | |
| **CD122** | BV421 | TM-β1 | BD Biosciences | 752988 | 1/50 | |
| **CD49a** | BV711 | Ha31/8 | BD Biosciences | 564863 | 1/100 | |
| **NK-1.1** | BUV615 | PK136 | BD Biosciences | 751111 | 1/100 | |
| **CD62L** | BUV805 | MEL-14 | BD Biosciences | 741924 | 1/400 | |
| **CD27** | BUV737 | LG.3A10 | BD Biosciences | 612831 | 1/100 | |
| **KLRG1** | PE-Cy5 | 2F1 | ThermoFisher | 15-5893-80 | 1/400 | |
| **CD8β** | BV510 | YTS156.7.7 | BioLegend | 126631 | 1/400 | For Lineage |
| **Ter-119** | BV785 | TER-119 | BioLegend | 116245 | 1/200 | For Lineage |
| **Ly-6G** | BV785 | 1A8 | BioLegend | 127645 | 1/200 | For Lineage |
| **F4-80** | BV785 | BM8 | BioLegend | 123141 | 1/200 | For Lineage |
| **CD11c** | BV785 | N418 | BioLegend | 117336 | 1/200 | For Lineage |
| **CD19** | BV785 | 6D5 | BioLegend | 115543 | 1/100 | For Lineage |
| **CD19** | AF700 | 1D3 | ThermoFisher | 56-0193-82 | 1/100 | For Lineage |
| **TCRγδ** | PE-CF594 | GL3 | BD Biosciences | 563532 | 1/200 | For Lineage |
| **TCRβ** | PE-CF594 | H57-597 | BD Biosciences | 562841 | 1/100 | For Lineage |
| **CD3e** | BUV395 | 145-2C11 | BD Bioscience | 563565 | 1/100 | For Lineage |
| **CD4** | BUV615 | RM4-5 | BD Biosciences | 751486 | 1/200 | For Lineage |
| **CD4** | BUV737 | GK1.5 | BD Bioscience | 612761 | 1/200 | For Lineage |
| **B220** | AF700 | RA3-6B2 | BioLegend | 103232 | 1/200 | |
| **CXCR6** | PE | SA051D1 | BioLegend | 151103 | 1/100 | |
| **CX3CR1** | FITC | SA011F11 | BioLegend | 149020 | 1/50 | |
| **CD127** | BV605 | A7R34 | BioLegend | 135041 | 1/50 | |
| **CD103** | BUV395 | M290 | BD Bioscience | 740238 | 1/100 | |
| **CD49b** | PE-Cy7 | DX5 | BioLegend | 108921 | 1/100 | |
| **Eomes** | PE | Dan11mag | ThermoFisher | 12-4875-82 | 1/100 | |
| **Rat IgG2a Isotype Control** | PE | eBR2a | ThermoFisher | 12-4321-42 | 1/100 | Eomes Isotype control |
| **Eomes** | AF647 | W17001A | Biolegend | 157703 | 1/100 | Intracellular |
| **CD31 (PECAM-1)** | FITC | 390 | ThermoFisher | 11-0311-82 | 1/100 | |
| **CD200R** | PE | OX-110 | BioLegend | 123907 | 1/100 | |
| **Ki-67** | BV605 | 16A8 | BioLegend | 652413 | 1/50 | Intracellular |
| **T-bet** | PE-Cy7 | 4B10 | ThermoFisher | 25-5825-82 | 1/50 | Intracellular |
| **IFN-γ** | BV605 | XMG1.2 | Biolegend | 505839 | 1/100 | Intracellular |
| **GM-CSF** | APC | MP1-22E9 | ThermoFisher | 17-7331-82 | 1/100 | Intracellular |
| **TNF-α** | PE | MP6-XT22 | ThermoFisher | 12-7321-81 | 1/100 | Intracellular |
| **TNF-α** | FITC | MP6-XT22 | BD Biosciences | 554418 | 1/100 | Intracellular |
| **Granzyme B** | PE-Cy7 | NGZB | ThermoFisher | 25-8898-80 | 1/100 | Intracellular |
| **Collagen IV** | Rabbit IgG (non-conjugated) | Polyclonal | Abcam | ab19808 | 1/100 | Used in 3D imaging |

| | | | | | | |
|---|---|---|---|---|---|---|
| **Secondary Rabbit-IgG** | Dylight488 | Polyclonal | ThermoFisher | SA5-10038 | 1/500 | Used in 3D imaging |
| **CD3e** | AF647 | 17A2 | Biolegend | 100209 | 1/100 | Used in 3D imaging |
| **CD3e** | AF647 | 17A2 | Biolegend | 100209 | 1/100 | Used in Live imaging |
| **TCRγδ** | APC | GL3 | Biolegend | 118116 | 1/50 | Used in Live imaging |
| **TCRβ** | APC | H57-597 | Biolegend | 159708 | 1/50 | Used in Live imaging |
| **CD11b** | FITC | M1/70 | ThermoFisher | 11-0112-82 | 1/50 | Used in Live imaging |
| **CD16/32** | purified | 2.4G2 | BD Biosciences | 553142 | 1/100 | For Fc-Receptor blocking |
| **Ly-6G** | FITC | 1A8 | BD Bioscience | 551460 | 1/100 | |
| **KLRG1** | BV605 | 2F1 | BioLegend | 138419 | 1/400 | |
| **KLRG1** | AF561 | 2F1 | ThermoFisher | 505-5893-82 | 1/400 | |
| **CD11c** | BV650 | N418 | BioLegend | 117339 | 1/100 | |
| **TCRβ** | BV711 | H57-597 | BioLegend | 109243 | 1/100 | |
| **MHC-II** | BV786 | 2G9 | BD Biosciences | 743875 | 1/800 | |
| **IL-18Ra** | AF647 | BG/IL18RA | Biolegend | 132903 | 1/100 | |
| **CD45** | PE | 30-F11 | BioLegend | 103105 | 1/300 | |
| **CD11b** | PE-Cy5 | M1/70 | ThermoFisher | 15-0112-81 | 1/800 | |
| **CD115** | PE-Cy7 | AFS98 | BioLegend | 135523 | 1/100 | |
| **CD115** | BV650 | AFS98 | BD Biosciences | 750891 | 1/100 | |
| **MHC-II** | AF700 | M5/114.15.2 | BioLegend | 107622 | 1/600 | |
| **CD19** | BV605 | 6D5 | BioLegend | 115540 | 1/200 | |
| **CD11b** | BV510 | M1/70 | BD Biosciences | 562950 | 1/600 | |
| **NKp46** | BUV737 | 29A1.4 | BD Bioscience | 612805 | 1/50 | |
| **CD8β** | FITC | YTS156.7.7 | Biolegend | 126606 | 1/200 | |
| **CX3CR1** | APC | SA011F11 | BioLegend | 149008 | 1/100 | |
| **CD117** | BB515 | 2B8 | BD Biosciences | 564481 | 1/100 | Not available from supplier anymore |
| **CD117** | FITC | 2B8 | BD Biosciences | 564481 | 1/100 | |
| **CD127** | BV421 | A7R34 | BioLegend | 135027 | 1/100 | |
| **CD25** | BV605 | PC61 | BD Bioscience | 563061 | 1/400 | |
| **CD4** | APC | GK1.5 | BioLegend | 100426 | 1/200 | |
| **CD44** | PE | IM7 | BD Biosciences | 553134 | 1/400 | |
| **CD28** | PE-Cy7 | E18 | Biolegend | 122014 | 1/100 | |
| **KLRG1** | AF647 | 2F1 | ThermoFisher | 51-5893-82 | 1/200 | |
| **NK-1.1** | PE-Cy7 | PK136 | BD biosciences | 552878 | 1/100 | |
| **CD4** | BV510 | RM4-5 | Biolegend | 100559 | 1/200 | |
| **NK-1.1** | APC | PK136 | BioLegend | 108710 | 1/100 | |
| **CD4** | FITC | GK1.5 | BD Biosciences | 557307 | 1/200 | |
| **CD122** | PerCP-eFluor710 | TM-b1 (TM-beta1) | ThermoFisher | 46-1222-82 | 1/100 | |
| **CD8β** | PE-Cy7 | YTS156.7.7 | Biolegend | 126616 | 1/200 | |
| **CD19** | APC | 1D3 | BioLegend | 152410 | 1/200 | |
| **CD11c** | APC | HL3 | BD Biosciences | 550261 | 1/200 | |
| **CD11b** | BV605 | M1/70 | BD Horizon | 563015 | 1/400 | |
| **MHC-II** | PE | M5/114.15.2 | ThermoFisher | 12-5321-81 | 1/600 | |
| **LY49H** | PE-Cy7 | 3D10 | BioLegend | 144714 | 1/200 | |

**Table S2: Total-seq antibodies (NTOC)**

| *TotalSeq* | *TotalSeq-A ID* | *Target* | *Clone* | *Isotype* |
|---|---|---|---|---|
| *A* | 0001 | CD4 | RM4-5 | Rat IgG2a, κ |
| *A* | 0002 | CD8a | 53-6.7 | Rat IgG2a, κ |
| *A* | 0003 | CD366 | RMT3-23 | Rat IgG2a, κ |
| *A* | 0004 | CD279 | RMP1-30 | Rat IgG2b, κ |
| *A* | 0012 | CD117 | 2B8 | Rat IgG2b, κ |
| *A* | 0013 | Ly-6C | HK1.4 | Rat IgG2c, κ |
| *A* | 0014 | CD11b | M1/70 | Rat IgG2b, κ |
| *A* | 0015 | Ly-6G | 1A8 | Rat IgG2a, κ |
| *A* | 0070 | CD49f | GoH3 | Rat IgG2a, κ |
| *A* | 0073 | CD44 | IM7 | Rat IgG2a, κ |
| *A* | 0074 | CD54 | YN1/1.7.4 | Rat IgG2b, κ |
| *A* | 0076 | CD15 | MC-480 | Mouse IgM, κ |
| *A* | 0077 | CD73 | TY/11.8 | Rat IgG1, κ |
| *A* | 0078 | CD49d | R1-2 | Rat IgG2b, κ |
| *A* | 0079 | CD200 | OX-90 | Rat IgG2a, κ |
| *A* | 0090 | IgG1, κ Isotype Ctrl | MOPC-21 | Mouse (BALB/c) IgG1, Œ∫ |
| *A* | 0091 | IgG2a, κ Isotype Ctrl | MOPC-173 | Mouse IgG2a, Œ∫ |
| *A* | 0092 | IgG2b, κ Isotype Ctrl | MPC-11 | Mouse IgG2b, Œ∫ |
| *A* | 0095 | IgG2b, κ Isotype Ctrl | RTK4530 | Rat IgG2b, Œ∫ |
| *A* | 0097 | CD25 | PC61 | Rat IgG1, λ |
| *A* | 0098 | CD135 | A2F10 | Rat IgG2a, κ |
| *A* | 0104 | CD102 | 3C4 (MIC2/4) | Rat IgG2a, κ |
| *A* | 0106 | CD11c | N418 | Armenian Hamster IgG |
| *A* | 0107 | CD21,CD35 | 7E9 | Rat IgG2a, κ |
| *A* | 0108 | CD23 | B3B4 | Rat IgG2a, κ |
| *A* | 0110 | CD43 | S11 | Rat IgG2b |
| *A* | 0112 | CD62L | MEL-14 | Rat IgG2a, κ |
| *A* | 0114 | F4/80 | BM8 | Rat IgG2a, κ |
| *A* | 0115 | FcεRIα | MAR-1 | Armenian Hamster IgG |
| *A* | 0117 | I-A/I-E | M5/114.15.2 | Rat IgG2b, κ |
| *A* | 0118 | NK-1.1 | PK136 | Mouse IgG2a, κ |
| *A* | 0119 | Siglec H | 551 | Rat IgG1, κ |
| *A* | 0120 | TCR β chain | H57-597 | Armenian Hamster IgG |
| *A* | 0121 | TCR γ/δ | GL3 | Armenian Hamster IgG |
| *A* | 0122 | TER-119 | TER-119 | Rat IgG2b, κ |
| *A* | 0130 | Ly-6A/E | D7 | Rat IgG2a, κ |
| *A* | 0171 | CD278 | C398.4A | Armenian Hamster IgG |
| *A* | 0184 | CD335 | 29A1.4 | Rat IgG2a, κ |
| *A* | 0190 | CD274 | MIH6 | Rat IgG2a, κ |
| *A* | 0191 | CD27 | LG.3A10 | Armenian Hamster IgG |

| | | | | |
|---|---|---|---|---|
| *A* | 0192 | CD20 | SA275A11 | Rat IgG2b, κ |
| *A* | 0193 | CD357 | DTA-1 | Rat IgG2b, λ |
| *A* | 0194 | CD137 | 17B5 | Syrian Hamster IgG |
| *A* | 0195 | CD134 | OX-86 | Rat IgG1, κ |
| *A* | 0197 | CD69 | H1.2F3 | Armenian Hamster IgG |
| *A* | 0198 | CD127 | A7R34 | Rat IgG2a, κ |
| *A* | 0200 | CD86 | GL-1 | Rat IgG2a, κ |
| *A* | 0201 | CD103 | 2E7 | Armenian Hamster IgG |
| *A* | 0203 | CD150 | TC15-12F12.2 | Rat IgG2a, λ |
| *A* | 0204 | CD28 | 37.51 | Syrian Hamster IgG |
| *A* | 0209 | TCR Vγ1.1 | 2.11 | Armenian Hamster IgG |
| *A* | 0210 | TCR Vγ3 | 536 | Syrian Hamster IgG |
| *A* | 0211 | TCR Vγ2 | UC3-10A6 | Armenian Hamster IgG |
| *A* | 0212 | CD24 | M1/69 | Rat IgG2b, κ |
| *A* | 0214 | Integrin β7 | FIB504 | Rat IgG2a, κ |
| *A* | 0225 | CD196 | 29-2L17 | Armenian Hamster IgG |
| *A* | 0226 | CD106 | 429 (MVCAM.A) | Rat IgG2a, κ |
| *A* | 0227 | CD122 | 5H4 | Rat IgG2a, κ |
| *A* | 0228 | CD183 | CXCR3-173 | Armenian Hamster IgG |
| *A* | 0229 | CD62P | RMP-1 | Mouse IgG2a, κ |
| *A* | 0230 | CD8b | YTS156.7.7 | Rat IgG2b, κ |
| *A* | 0232 | MAdCAM-1 | MECA-367 | Rat IgG2a, κ |
| *A* | 0235 | TCR Vβ8.1,8.2 | KJ16-133.18 | Rat IgG2a, κ |
| *A* | 0236 | IgG1, κ Isotype Ctrl | RTK2071 | Rat IgG1, Œ∫ |
| *A* | 0237 | IgG1, λ Isotype Ctrl | G0114F7 | Rat IgG1, Œª |
| *A* | 0238 | IgG2a, κ Isotype Ctrl | RTK2758 | Rat IgG2a, Œ∫ |
| *A* | 0240 | Rat IgG2c, κ Isotype Ctrl | RTK4174 | Rat IgG2c, Œ∫ |
| *A* | 0241 | IgG Isotype Ctrl | HTK888 | Armenian Hamster IgG |
| *A* | 0250 | KLRG1 | 2F1/KLRG1 | Syrian Hamster IgG |
| *A* | 0354 | TCR Vβ5.1, 5.2 | MR9-4 | Mouse IgG1, κ |
| *A* | 0376 | CD195 | HM-CCR5 | Armenian Hamster IgG |
| *A* | 0377 | CD197 | 4B12 | Rat IgG2a, κ |
| *A* | 0378 | CD223 | C9B7W | Rat IgG1, κ |
| *A* | 0379 | CD62E | RME-1/CD62E | Mouse IgG1, κ |
| *A* | 0381 | Panendothelial Cell Antigen | MECA-32 | Rat IgG2a, κ |
| *A* | 0388 | CD152 | UC10-4B9 | Armenian Hamster IgG |
| *A* | 0554 | CD309 | 89B3A5 | Rat IgG2a, κ |

**Table S3: Total-seq antibodies (Tissues)**

| *TotalSeq* | *TotalSeq-A ID* | *Target* | *Clone* | *Isotype* |
|---|---|---|---|---|
| *A* | 0001 | CD4 | RM4-5 | Rat IgG2a, κ |
| *A* | 0002 | CD8a | 53-6.7 | Rat IgG2a, κ |
| *A* | 0003 | CD366 | RMT3-23 | Rat IgG2a, κ |
| *A* | 0004 | CD279 | RMP1-30 | Rat IgG2b, κ |
| *A* | 0012 | CD117 | 2B8 | Rat IgG2b, κ |
| *A* | 0013 | Ly-6C | HK1.4 | Rat IgG2c, κ |
| *A* | 0014 | CD11b | M1/70 | Rat IgG2b, κ |
| *A* | 0015 | Ly-6G | 1A8 | Rat IgG2a, κ |
| *A* | 0070 | CD49f | GoH3 | Rat IgG2a, κ |
| *A* | 0074 | CD54 | YN1/1.7.4 | Rat IgG2b, κ |
| *A* | 0075 | CD90.2 | 30-H12 | Rat IgG2b, κ |
| *A* | 0076 | CD15 | MC-480 | Mouse IgM, κ |
| *A* | 0077 | CD73 | TY/11.8 | Rat IgG1, κ |
| *A* | 0078 | CD49d | R1-2 | Rat IgG2b, κ |
| *A* | 0079 | CD200 | OX-90 | Rat IgG2a, κ |
| *A* | 0090 | IgG1, κ Isotype Ctrl | MOPC-21 | Mouse (BALB/c) IgG1, Œ∫ |
| *A* | 0091 | IgG2a, κ Isotype Ctrl | MOPC-173 | Mouse IgG2a, Œ∫ |
| *A* | 0092 | IgG2b, κ Isotype Ctrl | MPC-11 | Mouse IgG2b, Œ∫ |
| *A* | 0093 | CD19 | 6D5 | Rat IgG2a, κ |
| *A* | 0095 | IgG2b, κ Isotype Ctrl | RTK4530 | Rat IgG2b, Œ∫ |
| *A* | 0097 | CD25 | PC61 | Rat IgG1, λ |
| *A* | 0098 | CD135 | A2F10 | Rat IgG2a, κ |
| *A* | 0103 | CD45R/B220 | RA3-6B2 | Rat IgG2a, κ |
| *A* | 0104 | CD102 | 3C4 (MIC2/4) | Rat IgG2a, κ |
| *A* | 0105 | CD115 | AFS98 | Rat IgG2a, κ |
| *A* | 0106 | CD11c | N418 | Armenian Hamster IgG |
| *A* | 0107 | CD21,CD35 | 7E9 | Rat IgG2a, κ |
| *A* | 0108 | CD23 | B3B4 | Rat IgG2a, κ |
| *A* | 0109 | CD16/32 | 93 | Rat IgG2a, λ |
| *A* | 0110 | CD43 | S11 | Rat IgG2b |
| *A* | 0111 | CD5 | 53-7.3 | Rat IgG2a, κ |
| *A* | 0112 | CD62L | MEL-14 | Rat IgG2a, κ |
| *A* | 0113 | CD93 | AA4.1 | Rat IgG2b, κ |
| *A* | 0114 | F4/80 | BM8 | Rat IgG2a, κ |
| *A* | 0115 | FcεRIα | MAR-1 | Armenian Hamster IgG |
| *A* | 0117 | I-A/I-E | M5/114.15.2 | Rat IgG2b, κ |
| *A* | 0118 | NK-1.1 | PK136 | Mouse IgG2a, κ |
| *A* | 0119 | Siglec H | 551 | Rat IgG1, κ |
| *A* | 0120 | TCR β chain | H57-597 | Armenian Hamster IgG |
| *A* | 0121 | TCR γ/δ | GL3 | Armenian Hamster IgG |
| *A* | 0122 | TER-119 | TER-119 | Rat IgG2b, κ |
| *A* | 0130 | Ly-6A/E | D7 | Rat IgG2a, κ |
| *A* | 0134 | CD146 | P1H12 | Mouse IgG1, κ |

| | | | | |
|---|---|---|---|---|
| *A* | 0171 | CD278 | C398.4A | Armenian Hamster IgG |
| *A* | 0173 | CD206 | C068C2 | Rat IgG2a, κ |
| *A* | 0182 | CD3 | 17A2 | Rat IgG2b, κ |
| *A* | 0184 | CD335 | 29A1.4 | Rat IgG2a, κ |
| *A* | 0190 | CD274 | MIH6 | Rat IgG2a, κ |
| *A* | 0191 | CD27 | LG.3A10 | Armenian Hamster IgG |
| *A* | 0192 | CD20 | SA275A11 | Rat IgG2b, κ |
| *A* | 0193 | CD357 | DTA-1 | Rat IgG2b, λ |
| *A* | 0194 | CD137 | 17B5 | Syrian Hamster IgG |
| *A* | 0195 | CD134 | OX-86 | Rat IgG1, κ |
| *A* | 0197 | CD69 | H1.2F3 | Armenian Hamster IgG |
| *A* | 0198 | CD127 | A7R34 | Rat IgG2a, κ |
| *A* | 0200 | CD86 | GL-1 | Rat IgG2a, κ |
| *A* | 0201 | CD103 | 2E7 | Armenian Hamster IgG |
| *A* | 0202 | CD64 | X54-5/7.1 | Mouse IgG1, κ |
| *A* | 0203 | CD150 | TC15-12F12.2 | Rat IgG2a, λ |
| *A* | 0204 | CD28 | 37.51 | Syrian Hamster IgG |
| *A* | 0209 | TCR Vγ1.1 | 2.11 | Armenian Hamster IgG |
| *A* | 0210 | TCR Vγ3 | 536 | Syrian Hamster IgG |
| *A* | 0211 | TCR Vγ2 | UC3-10A6 | Armenian Hamster IgG |
| *A* | 0212 | CD24 | M1/69 | Rat IgG2b, κ |
| *A* | 0214 | Integrin β7 | FIB504 | Rat IgG2a, κ |
| *A* | 0222 | ERK1 | W15133A | Rat IgG2a, κ |
| *A* | 0223 | RORg | 2F7-2 | Mouse IgG2a, κ |
| *A* | 0225 | CD196 | 29-2L17 | Armenian Hamster IgG |
| *A* | 0226 | CD106 | 429 (MVCAM.A) | Rat IgG2a, κ |
| *A* | 0227 | CD122 | 5H4 | Rat IgG2a, κ |
| *A* | 0228 | CD183 | CXCR3-173 | Armenian Hamster IgG |
| *A* | 0229 | CD62P | RMP-1 | Mouse IgG2a, κ |
| *A* | 0230 | CD8b | YTS156.7.7 | Rat IgG2b, κ |
| *A* | 0232 | MAdCAM-1 | MECA-367 | Rat IgG2a, κ |
| *A* | 0235 | TCR Vβ8.1,8.2 | KJ16-133.18 | Rat IgG2a, κ |
| *A* | 0236 | IgG1, κ Isotype Ctrl | RTK2071 | Rat IgG1, Œ∫ |
| *A* | 0237 | IgG1, λ Isotype Ctrl | G0114F7 | Rat IgG1, Œª |
| *A* | 0238 | IgG2a, κ Isotype Ctrl | RTK2758 | Rat IgG2a, Œ∫ |
| *A* | 0239 | IgG2a | #N/A | #N/A |
| *A* | 0240 | Rat IgG2c, κ Isotype Ctrl | RTK4174 | Rat IgG2c, Œ∫ |
| *A* | 0241 | IgG Isotype Ctrl | HTK888 | Armenian Hamster IgG |
| *A* | 0249 | IRF4 | IRF4.3E4 | Rat IgG1, κ |
| *A* | 0250 | KLRG1 | 2F1/KLRG1 | Syrian Hamster IgG |
| *A* | 0354 | TCR Vβ5.1, 5.2 | MR9-4 | Mouse IgG1, κ |

| | | | | |
|---|---|---|---|---|
| *A* | 0376 | CD195 | HM-CCR5 | Armenian Hamster IgG |
| *A* | 0377 | CD197 | 4B12 | Rat IgG2a, κ |
| *A* | 0378 | CD223 | C9B7W | Rat IgG1, κ |
| *A* | 0379 | CD62E | RME-1/CD62E | Mouse IgG1, κ |
| *A* | 0380 | CD90/CD90.1 | OX-7 | #N/A |
| *A* | 0381 | Panendothelial Cell Antigen | MECA-32 | Rat IgG2a, κ |
| *A* | 0388 | CD152 | UC10-4B9 | Armenian Hamster IgG |
| *A* | 0415 | P2RY12 | S16007D | Rat IgG2b, κ |
| *A* | 0416 | CD300LG | ZAQ5 | Rat IgG2a, κ |
| *A* | 0417 | CD163 | S15049I | Rat IgG2a, κ |
| *A* | 0421 | CD49b | HMα2 | Armenian Hamster IgG |
| *A* | 0422 | CD172a (SIRPα) | P84 | Rat IgG1, κ |
| *A* | 0424 | CD14 | Sa14-2 | Rat IgG2a, κ |
| *A* | 0426 | CD192 (CCR2) | SA203G11 | Rat IgG2b, κ |
| *A* | 0429 | CD48 | HM48-1 | Armenian Hamster IgG |
| *A* | 0434 | ReceptorD4 | #N/A | #N/A |
| *A* | 0435 | GABRB3 | #N/A | #N/A |
| *A* | 0437 | CD207_mh | 4C7 | Mouse IgG2a, κ |
| *A* | 0438 | KCC2 | #N/A | #N/A |
| *A* | 0439 | CD201 | RCR-16 | Rat IgG2a, κ |
| *A* | 0440 | CD169 | 3D6.112 | Rat IgG2a, κ |
| *A* | 0441 | CD71 | RI7217 | Rat IgG2a, κ |
| *A* | 0442 | Notch 1 | HMN1-12 | Armenian Hamster IgG |
| *A* | 0443 | CD41 | MWReg30 | Rat IgG1, κ |
| *A* | 0444 | CD184 | L276F12 | Rat IgG2b, κ |
| *A* | 0448 | CD204 | 1F8C33 | Rat IgG2a |
| *A* | 0449 | CD326 | G8.8 | Rat IgG2a, κ |
| *A* | 0450 | IgM | RMM-1 | Rat IgG2a, κ |
| *A* | 0551 | CD301a | LOM-8.7 | Rat IgG2a, κ |
| *A* | 0552 | CD304 | 3E12 | Rat IgG2a, κ |
| *A* | 0554 | CD309 | 89B3A5 | Rat IgG2a, κ |
| *A* | 0555 | CD36 | HM36 | Armenian Hamster IgG |
| *A* | 0556 | CD370 | 7H11 | Rat IgG1, κ |
| *A* | 0557 | CD38 | 90 | Rat IgG2a, κ |
| *A* | 0558 | CD55 | RIKO-3 | Armenian Hamster IgG |
| *A* | 0559 | CD63 | NVG-2 | Rat IgG2a, κ |
| *A* | 0560 | CD68 | FA-11 | Rat IgG2a |
| *A* | 0561 | CD79b | HM79-12 | Armenian Hamster IgG |
| *A* | 0562 | CD83 | Michel-19 | Rat IgG1, κ |
| *A* | 0563 | CX3CR1 | SA011F11 | Mouse IgG2a, κ |
| *A* | 0564 | Folate Receptor β | 10/FR2 | Rat IgG2a, κ |
| *A* | 0565 | MERTK | 2B10C42 | Rat IgG2a, κ |
| *A* | 0566 | CD301b | URA-1 | Rat IgG2a, λ |
| *A* | 0567 | Tim-4 | RMT4-54 | Rat IgG2a, κ |
| *A* | 0568 | XCR1 | ZET | Mouse IgG2b,κ |

| | | | | |
|---|---|---|---|---|
| *A* | 0570 | CD29 | HMβ1-1 | Armenian Hamster IgG |
| *A* | 0571 | IgD | 11-26c.2a | Rat IgG2a, κ |
| *A* | 0573 | CD140a | APA5 | Rat IgG2a, κ |
| *A* | 0595 | CD11a | M17/4 | Rat IgG2a, κ |
| *A* | 0596 | ESAM | 1G8/ESAM | Rat IgG2a, κ |
| *A* | 0807 | CD200R | OX-110 | Rat IgG2a, κ |
| *A* | 0808 | CD193 | J073E5 | Rat IgG2a, κ |
| *A* | 0809 | CD200R3 | Ba13 | Rat IgG2a, κ |
| *A* | 0810 | CD138 | 281-2 | Rat IgG2a, κ |
| *A* | 0811 | CD317 | 927 | Rat IgG2b, κ |
| *A* | 0812 | CD105 | MJ7/18 | Rat IgG2a, κ |
| *A* | 0813 | CD9 | MZ3 | Rat IgG2a, κ |
| *A* | 0824 | P2X7R | 1F11 | Rat IgG2b, κ |
| *A* | 0825 | CD371 | 5D3/CLEC12A | Rat IgG2a, κ |
| *A* | 0827 | CD22 | OX-97 | Rat IgG1, κ |
| *A* | 0834 | CD39 | Duha59 | Rat IgG2a, κ |
| *A* | 0835 | CD314 | CX5 | Rat IgG1, κ |
| *A* | 0836 | DR3 | 4C12 | Armenian Hamster IgG |
| *A* | 0837 | IL-33Rα | DIH9 | Rat IgG2a, κ |
| *A* | 0839 | Ly49H | 3D10 | Mouse IgG1, κ |
| *A* | 0841 | Ly49D | 4E5 | Rat IgG2a, κ |
| *A* | 0846 | CD185 | L138D7 | Rat IgG2b, κ |
| *A* | 0848 | TIGIT | 1G9 | Mouse IgG1, κ |
| *A* | 0849 | CD80 | 16-10A1 | Armenian Hamster IgG |
| *A* | 0850 | CD49a | HMα1 | Armenian Hamster IgG |
| *A* | 0851 | CD1d | 1B1 | Rat IgG2b, κ |
| *A* | 0852 | CD226 | 10E5 | Rat IgG2b, κ |
| *A* | 0857 | CD34 | HM34 | Armenian Hamster IgG |
| *A* | 0875 | TLR4 (CD284)/MD2 Complex | MTS510 | Rat IgG2a, κ |
| *A* | 0876 | CD300c/d | TX52 | Rat IgG2b, κ |
| *A* | 0877 | JAML | 4E10 | Armenian Hamster IgG |
| *A* | 0881 | CD272 | 6A6 | Armenian Hamster IgG |
| *A* | 0882 | PIR-A/B | 6C1 | Rat IgG1, κ |
| *A* | 0883 | CD26 | H194-112 | Rat IgG2a, κ |
| *A* | 0884 | DLL1 | HMD1-3 | Armenian Hamster IgG |
| *A* | 0885 | CD270 | HMHV-1B18 | Armenian Hamster IgG |
| *A* | 0890 | CD137L | TKS-1 | Rat IgG2a, κ |
| *A* | 0891 | ENPP1 | YE1/19.1 | Rat IgG2b, κ |
| *A* | 0892 | CD2 | RM2-5 | Rat IgG2b, λ |
| *A* | 0895 | Mac-2 | M3/38 | Rat IgG2a, κ |
| *A* | 0904 | CD31 | 390 | Rat IgG2a, κ |
| *A* | 0905 | CD107a | 1D4B | Rat IgG2a, κ |
| *A* | 0916 | CD124 | I015F8 | Rat IgG2b, κ |
| *A* | 0917 | CD95 (Fas) | SA367H8 | Mouse IgG1, κ |

**Table S4: Source data Fig 1F, NTOC Day 6 overview of cell types in lobes and supernatant**

| *Lobes count* | *Group-1 ILCs* | | | *Myeloid (Mo/Mac/Neu)* | | | *Developing T cells (DP/DN)* | | |
|---|---|---|---|---|---|---|---|---|---|
| *Vehicle* | 379 | 504 | 548 | 48905 | 46365 | 50670 | 169304 | 218277 | 137971 |
| *IL-12* | 960 | 1096 | 1092 | 135467 | 103488 | 123629 | 89851 | 64756 | 96514 |
| *IL-18* | 731 | 750 | 567 | 70694 | 74519 | 63706 | 118595 | 79645 | 64981 |
| *IL-12+IL-18* | 2709 | 3470 | 2595 | 86016 | 86059 | 91792 | 101158 | 121211 | 103519 |
| | *T cells (cTC/uTC)* | | | *DCs* | | | | | |
| *Vehicle* | 257861 | 289697 | 315969 | 8952 | 9055 | 11231 | | | |
| *IL-12* | 221177 | 144615 | 214513 | 7983 | 5359 | 6434 | | | |
| *IL-18* | 279058 | 341398 | 235461 | 12006 | 12316 | 5667 | | | |
| *IL-12+IL-18* | 167919 | 161391 | 158479 | 2999 | 1991 | 2259 | | | |
| | *B cells* | | | *Other* | | | | | |
| *Vehicle* | 2103 | 817 | 6399 | 28580 | 27615 | 34842 | | | |
| *IL-12* | 348 | 280 | 236 | 31583 | 19817 | 28087 | | | |
| *IL-18* | 731 | 1250 | 708 | 31325 | 32133 | 24179 | | | |
| *IL-12+IL-18* | 87 | 68 | 111 | 19361 | 22263 | 19469 | | | |

| *Lobes %* | *Group-1 ILCs* | | | *Myeloid (Mo/Mac/Neu)* | | | *Developing T cells (DP/DN)* | | |
|---|---|---|---|---|---|---|---|---|---|
| *Vehicle* | 0.073 | 0.085 | 0.098 | 9.476 | 7.828 | 9.087 | 32.806 | 36.85 | 24.742 |
| *IL-12* | 0.197 | 0.323 | 0.232 | 27.796 | 30.49 | 26.276 | 18.436 | 19.08 | 20.513 |
| *IL-18* | 0.143 | 0.138 | 0.143 | 13.777 | 13.749 | 16.117 | 23.112 | 14.69 | 16.44 |
| *IL-12+IL-18* | 0.712 | 0.875 | 0.686 | 22.621 | 21.707 | 24.269 | 26.603 | 30.57 | 27.37 |
| | *T cells (cTC/uTC)* | | | *DCs* | | | | | |
| *Vehicle* | 49.965 | 48.908 | 56.663 | 1.735 | 1.529 | 2.014 | | | |
| *IL-12* | 45.382 | 42.608 | 45.592 | 1.638 | 1.579 | 1.368 | | | |
| *IL-18* | 54.382 | 62.987 | 59.57 | 2.34 | 2.272 | 1.434 | | | |
| *IL-12+IL-18* | 44.16 | 40.709 | 41.901 | 0.789 | 0.502 | 0.597 | | | |
| | *B cells* | | | *Other* | | | | | |
| *Vehicle* | 0.407 | 0.138 | 1.148 | 5.538 | 4.662 | 6.248 | | | |
| *IL-12* | 0.071 | 0.083 | 0.05 | 6.48 | 5.839 | 5.969 | | | |
| *IL-18* | 0.143 | 0.231 | 0.179 | 6.105 | 5.928 | 6.117 | | | |
| *IL-12+IL-18* | 0.023 | 0.017 | 0.029 | 5.092 | 5.615 | 5.147 | | | |

| *Supernatant count* | *Group-1 ILCs* | | | *Myeloid (Mo/Mac/Neu)* | | | *Developing T cells (DP/DN)* | | |
|---|---|---|---|---|---|---|---|---|---|
| *Vehicle* | 730 | 880 | 846 | 23648 | 23743 | 34808 | 16776 | 19692 | 28349 |
| *IL-12* | 866 | 529 | 586 | 57489 | 42256 | 46303 | 4577 | 2328 | 3251 |
| *IL-18* | 4231 | 4097 | 3628 | 90784 | 87114 | 128923 | 16950 | 9726 | 12680 |
| *IL-12+IL-18* | 175858 | 156232 | 126249 | 326639 | 307862 | 271127 | 24397 | 44212 | 32937 |
| | *T cells (cTC/uTC)* | | | *DCs* | | | | | |
| *Vehicle* | 88085 | 93709 | 111424 | 1032 | 1278 | 2043 | | | |
| *IL-12* | 57581 | 34440 | 34295 | 325 | 212 | 176 | | | |
| *IL-18* | 110955 | 122742 | 90946 | 2266 | 1956 | 514 | | | |
| *IL-12+IL-18* | 51482 | 81915 | 66962 | 5511 | 4992 | 3367 | | | |
| | *B cells* | | | *Other* | | | | | |
| *Vehicle* | 238 | 138 | 846 | 11538 | 10820 | 16159 | | | |
| *IL-12* | 4 | 0 | 0 | 6104 | 3822 | 4325 | | | |
| *IL-18* | 117 | 56 | 74 | 24175 | 19846 | 18770 | | | |
| *IL-12+IL-18* | 58 | 47 | 79 | 19794 | 22539 | 22792 | | | |

| Supernatant % | Group-1 ILCs | | | Myeloid (Mo/Mac/Neu) | | | Developing T cells (DP/DN) | | |
|---|---|---|---|---|---|---|---|---|---|
| Vehicle | 0.514 | 0.586 | 0.435 | 16.648 | 15.801 | 17.899 | 11.81 | 13.105 | 14.577 |
| IL-12 | 0.682 | 0.633 | 0.659 | 45.286 | 50.554 | 52.064 | 3.605 | 2.785 | 3.655 |
| IL-18 | 1.696 | 1.668 | 1.42 | 36.389 | 35.479 | 50.452 | 6.794 | 3.961 | 4.962 |
| IL-12+IL-18 | 29.128 | 25.289 | 24.116 | 54.103 | 49.832 | 51.79 | 4.041 | 7.156 | 6.292 |
| | T cells (cTC/uTC) | | | DCs | | | | | |
| Vehicle | 62.011 | 62.365 | 57.295 | 0.726 | 0.851 | 1.051 | | | |
| IL-12 | 45.359 | 41.203 | 38.562 | 0.256 | 0.253 | 0.198 | | | |
| IL-18 | 44.475 | 49.989 | 35.59 | 0.908 | 0.797 | 0.201 | | | |
| IL-12+IL-18 | 8.527 | 13.259 | 12.791 | 0.913 | 0.808 | 0.643 | | | |
| | B cells | | | Other | | | | | |
| Vehicle | 0.168 | 0.092 | 0.435 | 8.123 | 7.201 | 8.309 | | | |
| IL-12 | 0.003 | 0 | 0 | 4.808 | 4.573 | 4.863 | | | |
| IL-18 | 0.047 | 0.023 | 0.029 | 9.69 | 8.083 | 7.345 | | | |
| IL-12+IL-18 | 0.01 | 0.008 | 0.015 | 3.279 | 3.648 | 4.354 | | | |

**Table S5: Source data Fig 1H, ILC1 kinetics in NTOC**

| ILC1 Kinetics | Vehicle Lobes | | | IL-12+IL-18 Lobes | | | Vehicle Supernatant | | | IL-12+IL-18 Supernatant | | |
|---|---|---|---|---|---|---|---|---|---|---|---|---|
| Day 1 | 2351 | 1762 | 2495 | 1900 | 2545 | 2271 | 117 | 704 | 612 | 34 | 391 | 73 |
| Day 2 | 937 | 1810 | 1535 | 8118 | 4491 | 6320 | 2124 | 3531 | 2118 | 36077 | 28050 | 22287 |
| Day 3 | 964 | 449 | 664 | 8723 | 7364 | 7367 | 2548 | 1548 | 1257 | 88297 | 114462 | 52007 |
| Day 6 | 431 | 664 | 483 | 2415 | 1829 | 1763 | 793 | 1091 | 1141 | 94579 | 122995 | 97140 |

**Table S6: Source data Fig S1D, CD45$^+$ cells in NTOC Day 6 in lobes and supernatant**

| | Lobes | | | Supernatant | | |
|---|---|---|---|---|---|---|
| Vehicle | 516082 | 592330 | 557631 | 142047 | 150260 | 194475 |
| IL-12 | 487370 | 339411 | 470504 | 126945 | 83587 | 88936 |
| IL-18 | 513139 | 542010 | 395268 | 249479 | 245536 | 255535 |
| IL-12+IL-18 | 380249 | 396453 | 378222 | 603740 | 617798 | 523512 |

**Table S7: Source data Fig 2B, YAC-1 cytotoxicity assay**

| YAC-1 Killing assay (E:T) | NTOC D6 ILC1s | | | | | | Splenic cNK_IL-12+IL-18 stimulation(18h) | | | | | |
|---|---|---|---|---|---|---|---|---|---|---|---|---|
| 0.1:1 | 13.4 | 15.3 | 14.4 | 15.3 | 11.83 | | 12.2 | 13.6 | 13.1 | 12.9 | 10.87 | |
| 1:1 | 14.9 | 15.8 | 18.2 | 16.5 | 14.77 | | 14.3 | 15.4 | 17.9 | 17.1 | 17.67 | |
| 2:1 | 19.1 | 18.8 | 22.4 | 18.8 | 18.6 | 22.5 | 18.7 | 19.6 | 19.7 | 20.1 | 31.6 | 22.6 |
| 4:1 | 17.3 | 22.4 | 25.4 | 22.8 | 27 | 32.97 | 32.3 | 30.9 | 27.7 | 30.1 | | 29.23 |
| 10:1 | 24.8 | 27 | 25.2 | 20.9 | 44.07 | 47.4 | 44 | 52.4 | 47 | 52.5 | | 45.2 |
| YAC-1 Killing assay (E:T) | Splenic cNK_No stimulation | | | | | | NTOC D6 CD4+Lin- | | | | | |
| 0.1:1 | 14.3 | 11.8 | 14.4 | 12.6 | 9.54 | | 13.5 | 13.9 | 14.1 | 16 | | |
| 1:1 | 13.1 | 12.9 | 14.3 | 14.8 | 13.13 | | 12.9 | 13.4 | 14 | 16.3 | | |
| 2:1 | 15.8 | 16.4 | 16 | 18.2 | 14.33 | 23.23 | 12.8 | 14.4 | 14.3 | 16.8 | | |
| 4:1 | 16.4 | 19.1 | 18.1 | 18.3 | 20.27 | 19.8 | 14 | 13.8 | 13.7 | 18.4 | | |
| 10:1 | 18.1 | 20.5 | 19.6 | 22.2 | 28.93 | 31.9 | 14.5 | 13.9 | 14.1 | 16 | | |

**Table S8: Source data Fig 2D, Cytokine measurements in NTOC supernatant Day 6**

| | | | | | | |
|---|---|---|---|---|---|---|
| *IFN-γ* | | | | | | |
| *Vehicle* | 58 | 21 | 12 | 10 | 81 | 186 |
| *IL-18* | 1323 | 1345 | 440 | 583 | 5439 | 1355 |
| *IL-12* | 27905 | 28047 | 27443 | 28934 | 27300 | 27767 |
| *IL-12+IL-18* | 29197 | 29851 | 28804 | 29843 | 28933 | 29717 |
| *TNF-α* | | | | | | |
| *Vehicle* | 181 | 321 | 215 | 144 | 379 | 409 |
| *IL-18* | 745 | 638 | 365 | 564 | 762 | 728 |
| *IL-12* | 947 | 595 | 759 | 1034 | 595 | 543 |
| *IL-12+IL-18* | 15068 | 17885 | 13665 | 15677 | 8257 | 3852 |
| *CCL3* | | | | | | |
| *Vehicle* | 183 | 197 | 137 | 219 | 393 | n/a |
| *IL-18* | 254 | 250 | 153 | 199 | 158 | 121 |
| *IL-12* | 92 | 45 | 101 | 165 | 62 | 87 |
| *IL-12+IL-18* | 17285 | 23515 | 19776 | 37780 | 7395 | 3317 |
| *GM-CSF* | | | | | | |
| *Vehicle* | 10 | 14 | 4 | 9 | 20 | 0.5 |
| *IL-18* | 87 | 125 | 48 | 74 | 119 | 68 |
| *IL-12* | 96 | 88 | 81 | 152 | 83 | 97 |
| *IL-12+IL-18* | 9186 | 9619 | 6141 | 6289 | 5021 | 1982 |

**Table S9: Source data Fig 3D, OP9-DL1 assay with ETP, DN2a, or ILC1 seeded cells**

| ***ETP seeding*** | *ILC1s (CD27+ KLRG1-)* | | *ILC1s (CD27- KLRG1-)* | | *ILC1s (KLRG1+ CD27-)* | | *DN cells (Lin-DN)* | | *DP and T cells (CD4/CD8b/CD3)* | |
|---|---|---|---|---|---|---|---|---|---|---|
| *IL-2+IL-15* | 64 | 262 | 34 | 63 | 2 | 0 | 3120 | 2456 | 6 | 4 |
| *IL-2+IL-7+IL-15* | 8288 | 6109 | 513 | 280 | 85 | 54 | 83065 | 90800 | 534 | 378 |
| *IL-2+IL-15+ IL-12+IL-18* | 5547 | 3875 | 481 | 558 | 126 | 162 | 34715 | 38634 | 264 | 286 |
| *IL-2+IL-7+IL-15+ IL-12+IL-18* | 18077 | 10252 | 2220 | 1100 | 1322 | 1481 | 32238 | 16659 | 1325 | 1596 |

| ***DN2a seeding*** | *ILC1s (CD27+ KLRG1-)* | | *ILC1s (CD27- KLRG1-)* | | *ILC1s (KLRG1+ CD27-)* | | *DN cells (Lin-DN)* | | *DP and T cells (CD4/CD8b/CD3)* | |
|---|---|---|---|---|---|---|---|---|---|---|
| *IL-2+IL-15* | 3 | 8 | 95 | 79 | 0 | 0 | 329 | 224 | 4657 | 4407 |
| *IL-2+IL-7+IL-15* | 375 | 280 | 121 | 92 | 3 | 0 | 28108 | 27321 | 11955 | 12250 |
| *IL-2+IL-15+ IL-12+IL-18* | 163 | 130 | 160 | 183 | 17 | 3 | 2094 | 3305 | 4730 | 5744 |
| *IL-2+IL-7+IL-15+ IL-12+IL-18* | 920 | 693 | 122 | 149 | 54 | 71 | 18484 | 14318 | 3633 | 3222 |

| *ILC1 seeding* | *ILC1s (CD27+ KLRG1-)* | | *ILC1s (CD27- KLRG1-)* | | *ILC1s (KLRG1+ CD27-)* | | *DN cells (Lin-DN)* | | *DP and T cells (CD4/CD8b/CD3)* | |
|---|---|---|---|---|---|---|---|---|---|---|
| *IL-2+IL-15* | 15283 | 16974 | 2412 | 2891 | 373 | 552 | 574 | 865 | 75 | 346 |
| *IL-2+IL-7+IL-15* | 38974 | 31098 | 9587 | 7829 | 1574 | 910 | 1424 | 1506 | 297 | 183 |
| *IL-2+IL-15+ IL-12+IL-18* | 3943 | 2737 | 3168 | 3077 | 19869 | 19879 | 4226 | 4578 | 810 | 565 |
| *IL-2+IL-7+IL-15+ IL-12+IL-18* | 4279 | 4893 | 3788 | 4617 | 23933 | 21753 | 3162 | 6277 | 1035 | 930 |

**Table S10: Source data Fig S3A, RAG2-/- OTI NTOC**

| | *Vehicle* | | | *IL-12+IL-18* | | |
|---|---|---|---|---|---|---|
| *WT* | 1185 | 783 | 3358 | 17897 | 35328 | 21582 |
| *RAG2-OTI* | 654 | 552 | 611 | 19511 | 14614 | 13386 |

**Table S11: Source data Fig 6C: Thymic-cellularity (MCMV)**

| | *Total live cells (thymus)* | | | | | | | | |
|---|---|---|---|---|---|---|---|---|---|
| *Sham* | 13133300 | 17634600 | 17370500 | 18028300 | 15156500 | 17443000 | 18453900 | 17540200 | 15759900 |
| *MCMV* | 15335600 | 8439600 | 13614900 | 10034700 | 15332700 | 17176200 | 17314300 | 17773400 | 10623600 |

**Table S12: Source data Fig 6D: Thymic-cellularity (IL-12+IL-18)**

| | *Total live cells (thymus)* | | | | | | | | |
|---|---|---|---|---|---|---|---|---|---|
| *Vehicle* | 11232700 | 10098200 | 10010100 | 13691700 | 10617700 | 16222100 | 13086500 | 10062800 | 17513600 |
| *IL-12+IL-18* | 9079300 | 6256600 | 9309100 | 4579700 | 4112500 | 6876700 | 3215100 | 6145900 | |

**Table S13: Source data Fig 6E: Thymic-derived ILC1s (MCMV)**

| | *Total number of thymic ILC1s* | | | | | | | | |
|---|---|---|---|---|---|---|---|---|---|
| *Sham* | 2997.882 | 2605.575 | 2523.962 | 2273.475 | 2093.16 | 2399.007 | 2806.432 | 1891.188 | |
| *MCMV* | 2300.34 | 1265.94 | 1633.788 | 1103.817 | 1310.946 | 3435.24 | 2077.716 | 1955.074 | 772.3357 |

**Table S14: Source data Fig 6F: Thymic-derived ILC1s (IL-12+IL-18)**

| | *Total number of thymic ILC1s* | | | | | | | |
|---|---|---|---|---|---|---|---|---|
| *Vehicle* | 1120 | 1920 | 1400 | 1640 | 1270 | 1530 | 1830 | |
| *IL-12+IL-18* | 3450 | 3000 | 3630.549 | 962 | 2140 | 1240 | 932 | 1040 |

**Table S15: Source data Fig 6G: KLRG1 MFI in Thymic-derived ILC1s (MCMV)**

| | *KLRG1 MFI in thymic resident ILC1s* | | | | | | | | |
|---|---|---|---|---|---|---|---|---|---|
| *Sham* | 1270 | 1336 | 1242 | 1194 | 1401 | 1310 | 1339 | 1336 | |
| *MCMV* | 1600 | 1378 | 1499 | 1413 | 1389 | 1453 | 1499 | 1618 | 1466 |

**Table S16: Source data Fig 6H: KLRG1 MFI in Thymic-derived ILC1s (IL-12+IL-18)**

| | *KLRG1 MFI in thymic resident ILC1s* | | | | | | | |
|---|---|---|---|---|---|---|---|---|
| *Vehicle* | 1340 | 1390 | 1340 | 1300 | 1240 | 1370 | 1120 | |
| *IL-12+IL-18* | 1560 | 1490 | 1397 | 1540 | 1420 | 1490 | 1370 | 1450 |

**Table S17: Source data Fig 6I: CXCR6 MFI in Thymic-derived ILC1s (MCMV)**

| | *CXCR6 MFI in thymic resident ILC1s* | | | | | | | | |
|---|---|---|---|---|---|---|---|---|---|
| *Sham* | 1664 | 1828 | 1699 | 1600 | 1874 | 1913 | 1624 | 1664 | |
| *MCMV* | 1935 | 1794 | 2017 | 1888 | 1709 | 1686 | 2164 | 2103 | 1913 |

**Table S18: Source data Fig 6J: CXCR6 MFI in Thymic-derived ILC1s (IL-12+IL-18)**

| | *CXCR6 MFI in thymic resident ILC1s* | | | | | | | |
|---|---|---|---|---|---|---|---|---|
| *Vehicle* | 1630 | 1700 | 1910 | 1780 | 1460 | 2090 | 1320 | |
| *IL-12+IL-18* | 2720 | 2410 | 2280 | 2530 | 2360 | 2820 | 2760 | 2580 |

**Table S19: Source data Fig S6G: Ly49H expressing Group-1 ILCs**

| | *(%) Ly49H+ Group-1 ILCs* | | | | | | | | |
|---|---|---|---|---|---|---|---|---|---|
| *Sham* | 1.67 | 1.17 | 1.64 | 1.68 | 3.38 | 1.1 | 2.13 | 2.58 | |
| *MCMV* | 1.61 | 1.62 | 2.01 | 1.59 | 2.69 | 1.73 | 1.42 | 0.67 | 1.14 |

| | *(%) Ly49H+ Group-1 ILCs* | | | | | | | |
|---|---|---|---|---|---|---|---|---|
| *Vehicle* | 1.26 | 1.63 | 1.28 | 1.85 | 1.79 | 1.12 | | |
| *IL-12+IL-18* | 1.06 | 1.05 | 1.52 | 1.26 | 1.03 | 1.55 | 2.54 | 1.58 |

**Table S20: Source data Fig 7C: Thymic graft-derived ILC1s (KLRG1 and CD27 expression**

| *Thymic-derived ILC1s* | *Spleen IL-2+IL-12+IL-18* | | | | *Spleen IL-2* | | | |
|---|---|---|---|---|---|---|---|---|
| *CD27+KLRG1- ILC1s* | 1986 | 3316 | 1933 | 1892 | 2104 | 1807 | 3491 | |
| *CD27-KLRG1- ILC1s* | 545 | 1064 | 730 | 523 | 301 | 210 | 452 | |
| *KLRG1+ ILC1s* | 389 | 901 | 773 | 1087 | 429 | 210 | 123 | |

| *Thymic-derived ILC1s* | *PEC IL-2+IL-12+IL-18* | | | | | | | *PEC IL-2* | | | | | |
|---|---|---|---|---|---|---|---|---|---|---|---|---|---|
| *CD27+KLRG1- ILC1s* | 363 | 503 | 490 | 1404 | 1527 | 843 | 95 | 556 | 926 | 344 | 225 | 1371 | 1022 |
| *CD27-KLRG1- ILC1s* | 4881 | 4957 | 3224 | 4146 | 5653 | 3651 | 1008 | 376 | 815 | 377 | 180 | 1270 | 761 |
| *KLRG1+ ILC1s* | 17062 | 7161 | 10627 | 10743 | 8360 | 8842 | 6003 | 161 | 673 | 228 | 22 | 2440 | 227 |

| *Thymic-derived ILC1s* | *Liver IL-2+IL-12+IL-18* | | | | | | | *Liver IL-2* | | | | | |
|---|---|---|---|---|---|---|---|---|---|---|---|---|---|
| *CD27+KLRG1- ILC1s* | 72 | 431 | 210 | 289 | 507 | 333 | 117 | 118 | 287 | 165 | 114 | 167 | |
| *CD27-KLRG1- ILC1s* | 122 | 186 | 189 | 410 | 707 | 491 | 234 | 37 | 73 | 146 | 105 | 198 | |
| *KLRG1+ ILC1s* | 1073 | 917 | 814 | 670 | 760 | 546 | 693 | 95 | 150 | 35 | 30 | 34 | |

**Table S21: Source data Fig 7E: Graft-derived KLRG1+ ILC1s : CD4 T cells (Ratio)**

| | *IL-2+IL-12+IL-18* | | | | | | | *IL-2* | | | | | |
|---|---|---|---|---|---|---|---|---|---|---|---|---|---|
| *Spleen* | 0.0018 | 0.0033 | 0.0046 | 0.0025 | | | | 0.0014 | 0.0005 | 0.0004 | | | |
| *PC* | 3.4673 | 2.1812 | 3.9831 | 0.3015 | 0.3007 | 0.2283 | 0.4456 | 0.0381 | 0.3235 | 0.1659 | 0.003 | 0.1293 | 0.0146 |
| *Liver* | 0.722 | 0.4951 | 1.1493 | 0.0719 | 0.218 | 0.0632 | 0.1855 | 0.1715 | 0.0823 | 0.0078 | 0.0169 | 0.0101 | |

**Table S22: Source data Fig 7F: Graft-derived ILC1s (%) expression of IFN-y**

| | *IL-2+IL-12+IL-18* | | | | | | *IL-2* | | | | | |
|---|---|---|---|---|---|---|---|---|---|---|---|---|
| *Spleen* | 60 | 59.6 | 47.7 | 42.9 | 40 | 11.1 | 20.9 | 20.9 | 13.3 | 28 | 37.5 | 25 |
| *PC* | 91.1 | 65.4 | 39 | 77.2 | 73.7 | 82.6 | 2 | 19 | 3.45 | 0 | 6.06 | 0 |
| *Liver* | 26.9 | 24.6 | 30.2 | 14.4 | 4.49 | 12.5 | 0.87 | 0.71 | 2.04 | 1.41 | 0 | 1.19 |

**Table S23: Source data Fig 7G: Graft-derived ILC1s (%) expression of TNF-a**

| | *IL-2+IL-12+IL-18* | | | | | | *IL-2* | | | | | |
|---|---|---|---|---|---|---|---|---|---|---|---|---|
| *Spleen* | 56 | 51.1 | 43.1 | 42.9 | 0 | 22.2 | 12.8 | 13.4 | 15.6 | 4 | 0 | 0 |
| *PC* | 21.3 | 18.5 | 17.8 | 18 | 33.6 | 35.8 | 0 | 10.3 | 0 | 0 | 0 | 0 |
| *Liver* | 11.6 | 10.4 | 15.5 | 4.02 | 1.28 | 2.27 | 0 | 2.86 | 2.04 | 1.41 | 0 | 0 |

**Table S24: Source data Fig S7C: Thymic-derived CD27+KLRG1- ILC1s in periphery**

| | *IL-2+IL-12+IL-18* | | | | | | | *IL-2* | | | | | |
|---|---|---|---|---|---|---|---|---|---|---|---|---|---|
| *Spleen* | 1986 | 3316 | 1933 | 1892 | | | | 2104 | 1807 | 3491 | | | |
| *PC* | 363 | 503 | 490 | 1404 | 1527 | 843 | 95 | 556 | 926 | 344 | 225 | 1371 | 1022 |
| *Liver* | 72 | 431 | 210 | 289 | 507 | 333 | 117 | 118 | 287 | 165 | 114 | 167 | |

**Table S25: Source data Fig S7D: Thymic-derived KLRG1+ ILC1s in periphery**

| | *IL-2+IL-12+IL-18* | | | | | | | *IL-2* | | | | | |
|---|---|---|---|---|---|---|---|---|---|---|---|---|---|
| *Spleen* | 389 | 901 | 773 | 1087 | | | | 429 | 210 | 123 | | | |
| *PC* | 17062 | 7161 | 10627 | 10743 | 8360 | 8842 | 6003 | 161 | 673 | 228 | 22 | 2440 | 227 |
| *Liver* | 1073 | 917 | 814 | 670 | 760 | 546 | 693 | 95 | 150 | 35 | 30 | 34 | |

**Table S26: Source data Fig S7E: Thymic-derived ILC1s - thymus graft**

| | IL-2+IL-12+IL-18 | | | | IL-2 | | |
|---|---|---|---|---|---|---|---|
| *Thymus graft* | 332 | 40 | 384 | 389 | 783 | 273 | 638 |

**Table S27: Source data Fig S7F: Thymic-derived CD4 T cells**

| | IL-2+IL-12+IL-18 | | | | | | | IL-2 | | | | | |
|---|---|---|---|---|---|---|---|---|---|---|---|---|---|
| *Spleen* | 211836 | 277036 | 167354 | 441506 | | | | 315243 | 395294 | 326407 | | | |
| *PC* | 4921 | 3283 | 2668 | 35629 | 27799 | 38737 | 13471 | 4229 | 2079 | 1376 | 7422 | 18875 | 15565 |
| *Liver* | 1486 | 1852 | 708 | 9324 | 3487 | 8645 | 3736 | 553 | 1818 | 4478 | 1779 | 3361 | |

**Table S28: Source data Fig S7G: Graft-derived ILC1s : CD4 T cells (Ratio)**

| | IL-2+IL-12+IL-18 | | | | | | | IL-2 | | | | | |
|---|---|---|---|---|---|---|---|---|---|---|---|---|---|
| *Spleen* | 0.0138 | 0.0189 | 0.02 | 0.0082 | | | | 0.009 | 0.0055 | 0.0125 | | | |
| *PEC* | 4.5329 | 3.8443 | 5.3752 | 0.4629 | 0.5625 | 0.3538 | 0.5454 | 0.2586 | 1.161 | 0.6901 | 0.0546 | 0.2885 | 0.1285 |
| *Liver* | 0.8603 | 0.8333 | 1.7175 | 0.1488 | 0.5698 | 0.1614 | 0.2912 | 0.4521 | 0.2803 | 0.077 | 0.1372 | 0.1166 | |

## Supplementary Movies

### Movie S1: Live imaging of Thymic ILC1 exiting into the culture media

Live confocal imaging of neonatal thymus organ culture samples (Day 4 of culture). Thymus derived from P0.5 *Ncr1*-tdTomato neonatal mice. The lobes were either treated with Vehicle (left) or IL-12+IL-18 (right). Images taken every 30 minutes. Markers: Green (*Ncr1*-tdTomato), Red (CD3e/TCRβ/TCRγδ), and Blue (Hoechst). The arrows indicates the thymus exiting cells. The movie is representative of $n$ = 10 biological replicates from two independent experiments.

## Excel Tables

### Excel Table S1: Source data file

Source data for individual graphs and figures.

**REFERENCES AND NOTES**


1. M. M. Gherardi, J. C. Ramírez, M. Esteban, IL-12 and IL-18 act in synergy to clear vaccinia virus infection: Involvement of innate and adaptive components of the immune system. *J. Gen. Virol.* **84** (Pt. 8), 1961–1972 (2003).

2. G. C. Pien, A. R. Satoskar, K. Takeda, S. Akira, C. A. Biron, Cutting edge: Selective IL-18 requirements for induction of compartmental IFN-γ responses during viral infection. *J. Immunol.* **165**, 4787–4791 (2000).

3. T. Vanden Berghe, D. Demon, P. Bogaert, B. Vandendriessche, A. Goethals, B. Depuydt, M. Vuylsteke, R. Roelandt, E. Van Wonterghem, J. Vandenbroecke, S. M. Choi, E. Meyer, S. Krautwald, W. Declercq, N. Takahashi, A. Cauwels, P. Vandenabeele, Simultaneous targeting of IL-1 and IL-18 is required for protection against inflammatory and septic shock. *Am. J. Respir. Crit. Care Med.* **189**, 282–291 (2014).

4. S. Mera, D. Tatulescu, C. Cismaru, C. Bondor, A. Slavcovici, V. Zanc, D. Carstina, M. Oltean, Multiplex cytokine profiling in patients with sepsis. *APMIS.* **119**, 155–163 (2011).

5. N. Bourgon, W. Fitzgerald, H. Aschard, J. F. Magny, T. Guilleminot, J. Stirnemann, R. Romero, Y. Ville, L. Margolis, M. Leruez-Ville, Cytokine profiling of amniotic fluid from congenital cytomegalovirus infection. *Viruses* **14**, 2145 (2022).

6. J. Renneson, B. Dutta, S. Goriely, B. Danis, S. Lecomte, J. F. Laes, Z. Tabi, M. Goldman, A. Marchant, IL-12 and type I IFN response of neonatal myeloid DC to human CMV infection. *Eur. J. Immunol.* **39**, 2789–2799 (2009).

7. U. S. Akpan, L. S. Pillarisetty, Congenital cytomegalovirus infection, in *StatPearls* (StatPearls, 2022); www.ncbi.nlm.nih.gov/books/NBK541003/.

8. E. A. Osterholm, M. R. Schleiss, Impact of breast milk-acquired cytomegalovirus infection in premature infants: Pathogenesis, prevention, and clinical consequences? *Rev. Med. Virol.* **30**, 1–11 (2020).

9. F. Namba, R. Nakagawa, M. Haga, S. Yoshimoto, Y. Tomobe, K. Okazaki, K. Nakamura, Y. Seki, S. Kitamura, T. Shimokaze, H. Ikegami, K. Nishida, S. Mori, K. Tamai, J. Ozawa, K. Tanaka, N. Miyahara, Cytomegalovirus-related sepsis-like syndrome in very premature infants in Japan. *Pediatr. Int.* **64**, e14994 (2022).

10. Y. Kong, Y. Li, W. Zhang, S. Yuan, R. Winkler, U. Kröhnert, J. Han, T. Lin, Y. Zhou, P. Miao, B. Wang, J. Zhang, Z. Yu, Y. Zhang, C. Kosan, H. Zeng, Sepsis-induced thymic atrophy is associated with defects in early lymphopoiesis. *Stem Cells* **34**, 2902–2915 (2016).

11. M. Luo, L. Xu, Z. Qian, X. Sun, Infection-associated thymic atrophy. *Front. Immunol.* **12**, 652538 (2021).

12. A. R. Ansari, H. Liu, Acute thymic involution and mechanisms for recovery. *Arch. Immunol. Ther. Exp.* ***65***, 401–420 (2017).

13. E. N. Lee, J. K. Park, J.-R. Lee, S.-O. Oh, S.-Y. Baek, B.-S. Kim, S. Yoon, Characterization of the expression of cytokeratins 5, 8, and 14 in mouse thymic epithelial cells during thymus regeneration following acute thymic involution. *Anat. Cell Biol.* **44**, 14–24 (2011).

14. G. Pearse, Normal structure, function and histology of the thymus. *Toxicol. Pathol.* **34**, 504–514 (2006).

15. C. Berthault, T. Larcher, S. Härtle, J. F. Vautherot, L. Trapp-Fragnet, C. Denesvre, Atrophy of primary lymphoid organs induced by Marek's disease virus during early infection is associated with increased apoptosis, inhibition of cell proliferation and a severe B-lymphopenia. *Vet. Res.* **49**, 31 (2018).

16. L. Ducimetière, G. Lucchiari, G. Litscher, M. Nater, L. Heeb, N. G. Nuñez, L. Wyss, D. Burri, M. Vermeer, J. Gschwend, A. E. Moor, B. Becher, M. van den Broek, S. Tugues, Conventional NK cells and tissue-resident ILC1s join forces to control liver metastasis. *Proc. Natl. Acad. Sci. U.S.A.* **118**, e2026271118 (2021).

17. J. P. Shannon, S. M. Vrba, G. V. Reynoso, E. Wynne-Jones, O. Kamenyeva, C. S. Malo, C. R. Cherry, D. T. McManus, H. D. Hickman, Group 1 innate lymphoid-cell-derived interferon-γ maintains anti-viral vigilance in the mucosal epithelium. *Immunity* **54**, 276–290.e5 (2021).

18. O. El Weizman, N. M. Adams, I. S. Schuster, C. Krishna, Y. Pritykin, C. Lau, M. A. Degli-Esposti, C. S. Leslie, J. C. Sun, T. E. O'Sullivan, ILC1 confer early host protection at initial sites of viral infection. *Cell* **171**, 795–808.e12 (2017).

19. C. Sparano, D. Solís-Sayago, A. Vijaykumar, C. Rickenbach, M. Vermeer, F. Ingelfinger, G. Litscher, A. Fonseca, C. Mussak, M. Mayoux, C. Friedrich, C. Nombela-Arrieta, G. Gasteiger, B. Becher, S. Tugues, Embryonic and neonatal waves generate distinct populations of hepatic ILC1s. *Sci. Immunol.* **7**, eabo6641 (2022).

20. Y. Chen, X. Wang, X. Hao, B. Li, W. Tao, S. Zhu, K. Qu, H. Wei, R. Sun, H. Peng, Z. Tian, Ly49E separates liver ILC1s into embryo-derived and postnatal subsets with different functions. *J. Exp. Med.* **219**, e20211805 (2022).

21. N. Lopes, J. Galluso, B. Escalière, S. Carpentier, Y. M. Kerdiles, E. Vivier, Tissue-specific transcriptional profiles and heterogeneity of natural killer cells and group 1 innate lymphoid cells. *Cell Rep. Med.* **3**, 100812 (2022).

22. T. Kogame, G. Egawa, T. Nomura, K. Kabashima, Waves of layered immunity over innate lymphoid cells. *Front. Immunol.* **13**, 957711 (2022).

23. C. A. J. J. Vosshenrich, M. E. García-Ojeda, S. I. Samson-Villéger, V. Pasqualetto, L. Enault, O. R.-L. Le Goff, E. Corcuff, D. Guy-Grand, B. Rocha, A. Cumano, L. Rogge, S. Ezine, J. P. Di Santo, A thymic pathway of mouse natural killer cell development characterized by expression of GATA-3 and CD127. *Nat. Immunol.* **7**, 1217–1224 (2006).

24. S. Gabrielli, M. Sun, A. Bell, E. C. Zook, R. F. de Pooter, L. Zamai, B. L. Kee, Murine thymic NK cells are distinct from ILC1s and have unique transcription factor requirements. *Eur. J. Immunol.* **47**, 800–805 (2017).

25. C. L. Vargas, J. Poursine-Laurent, L. Yang, W. M. Yokoyama, Development of thymic NK cells from double negative 1 thymocyte precursors. *Blood* **118**, 3570–3578 (2011).

26. M. Cordes, K. Canté-Barrett, E. B. van den Akker, F. A. Moretti, S. M. Kiełbasa, S. A. Vloemans, L. Garcia-Perez, C. Teodosio, J. J. M. van Dongen, K. Pike-Overzet, M. J. T. Reinders, F. J. T. Staal, Single-cell immune profiling reveals thymus-seeding populations, T cell commitment, and multilineage development in the human thymus. *Sci. Immunol.* **7**, eade0182 (2022).

27. T. M. Schmitt, M. Ciofani, H. T. Petrie, J. C. Zúñiga-Pflücker, J. Carlos Zúñiga-Pflücker, Maintenance of T cell specification and differentiation requires recurrent Notch receptor-ligand interactions. *J. Exp. Med.* **200**, 469–479 (2004).

28. M. Lavaert, K. L. Liang, N. Vandamme, J. E. Park, J. Roels, M. S. Kowalczyk, B. Li, O. Ashenberg, M. Tabaka, D. Dionne, T. L. Tickle, M. Slyper, O. Rozenblatt-Rosen, B. Vandekerckhove, G. Leclercq, A. Regev, P. Van Vlierberghe, M. Guilliams, S. A. Teichmann, Y. Saeys, T. Taghon, Integrated scRNA-seq identifies human postnatal thymus seeding progenitors and regulatory dynamics of differentiating immature thymocytes. *Immunity* **52**, 1088–1104.e6 (2020).

29. R. Elsaid, S. Meunier, O. Burlen-Defranoux, F. Soares-da-Silva, T. Perchet, L. Iturri, L. Freyer, P. Vieira, P. Pereira, R. Golub, A. Bandeira, E. G. Perdiguero, A. Cumano, A wave of bipotent T/ILC-restricted progenitors shapes the embryonic thymus microenvironment in a time-dependent manner. *Blood* **137**, 1024–1036 (2021).

30. V. Stokic-Trtica, A. Diefenbach, C. S. N. Klose, NK cell development in times of innate lymphoid cell diversity. *Front. Immunol.* **11**, 813 (2020).

31. C. S. N. Klose, M. Flach, L. Möhle, L. Rogell, T. Hoyler, K. Ebert, C. Fabiunke, D. Pfeifer, V. Sexl, D. Fonseca-Pereira, R. G. Domingues, H. Veiga-Fernandes, S. J. Arnold, M. Busslinger, I. R. Dunay, Y. Tanriver, A. Diefenbach, Differentiation of type 1 ILCs from a common progenitor to all helper-like innate lymphoid cell lineages. *Cell* **157**, 340–356 (2014).

32. Y. Gao, F. Souza-Fonseca-Guimaraes, T. Bald, S. S. Ng, A. Young, S. F. Ngiow, J. Rautela, J. Straube, N. Waddell, S. J. Blake, J. Yan, L. Bartholin, J. S. Lee, E. Vivier, K. Takeda, M. Messaoudene, L. Zitvogel, M. W. L. Teng, G. T. Belz, C. R. Engwerda, N. D. Huntington, K. Nakamura, M. Hölzel, M. J. Smyth, Tumor immunoevasion by the conversion of effector NK cells into type 1 innate lymphoid cells. *Nat. Immunol.* **18**, 1004–1015 (2017).

33. S. Flommersfeld, J. P. Böttcher, J. Ersching, M. Flossdorf, P. Meiser, L. O. Pachmayr, J. Leube, I. Hensel, S. Jarosch, Q. Zhang, M. Z. Chaudhry, I. Andrae, M. Schiemann, D. H. Busch, L. Cicin-Sain, J. C. Sun, G. Gasteiger, G. D. Victora, T. Höfer, V. R. Buchholz, S. Grassmann, Fate mapping of single NK cells identifies a type 1 innate lymphoid-like lineage that bridges innate and adaptive recognition of viral infection. *Immunity* **54**, 2288–2304.e7 (2021).

34. E. Park, S. Patel, Q. Wang, P. Andhey, K. Zaitsev, S. Porter, M. Hershey, M. Bern, B. Plougastel-Douglas, P. Collins, M. Colonna, K. M. Murphy, E. Oltz, M. Artyomov, L. D. Sibley, W. M. Yokoyama, *Toxoplasma gondii* infection drives conversion of NK cells into ILC1-like cells. *eLife* **8**, e47605 (2019).

35. M. G. Constantinides, B. D. McDonald, P. A. Verhoef, A. Bendelac, A committed precursor to innate lymphoid cells. *Nature* **508**, 397–401 (2014), .

36. C. Daussy, F. Faure, K. Mayol, S. Viel, G. Gasteiger, E. Charrier, J. Bienvenu, T. Henry, E. Debien, U. A. Hasan, J. Marvel, K. Yoh, S. Takahashi, I. Prinz, S. De Bernard, L. Buffat, T. Walzer, T-bet and Eomes instruct the development of two distinct natural killer cell lineages in the liver and in the bone marrow. *J. Exp. Med.* **211**, 563–577 (2014).

37. S. M. Gordon, J. Chaix, L. J. Rupp, J. Wu, S. Madera, J. C. Sun, T. Lindsten, S. L. Reiner, The transcription factors T-bet and Eomes control key checkpoints of natural killer cell maturation. *Immunity* **36**, 55–67 (2012).

38. C. Friedrich, R. L. R. E. Taggenbrock, R. Doucet-Ladevèze, G. Golda, R. Moenius, P. Arampatzi, N. A. M. Kragten, K. Kreymborg, M. Gomez de Agüero, W. Kastenmüller, A. E. Saliba, D. Grün, K. P. J. M. van Gisbergen, G. Gasteiger, Effector differentiation downstream of

lineage commitment in ILC1s is driven by Hobit across tissues. *Nat. Immunol.* **22**, 1256–1267 (2021).

39. M. Malaisé, J. Rovira, P. Renner, E. Eggenhofer, M. Sabet-Baktach, M. Lantow, S. A. Lang, G. E. Koehl, S. A. Farkas, M. Loss, A. Agha, J. M. Campistol, H. J. Schlitt, E. K. Geissler, A. Kroemer, KLRG1$^{+}$ NK cells protect T-bet-deficient mice from pulmonary metastatic colorectal carcinoma. *J. Immunol.* **192**, 1954–1961 (2014).

40. K. Nakatani, K. Kaneda, S. Seki, Y. Nakajima, Pit cells as liver-associated natural killer cells: Morphology and function. *Med. Electron Microsc.* **37**, 29–36 (2004).

41. S. B. Shin, K. M. McNagny, ILC-you in the thymus: A fresh look at innate lymphoid cell development. *Front. Immunol.* **12**, 681110 (2021).

42. J. Xiong, Y. Zhao, Y. Lin, L. Chen, Q. Weng, C. Shi, X. Liu, Y. Geng, L. Liu, J. Wang, M. Zhang, Identification and characterization of innate lymphoid cells generated from pluripotent stem cells. *Cell Rep.* **41**, 111569 (2022).

43. M. T. Orr, J. C. Sun, D. G. T. Hesslein, H. Arase, J. H. Phillips, T. Takai, L. L. Lanier, Ly49H signaling through DAP10 is essential for optimal natural killer cell responses to mouse cytomegalovirus infection. *J. Exp. Med.* **206**, 807–817 (2009).

44. E. Narni-Mancinelli, J. Chaix, A. Fenis, Y. M. Kerdiles, N. Yessaad, A. Reynders, C. Gregoire, H. Luche, S. Ugolini, E. Tomasello, T. Walzer, E. Vivier, Fate mapping analysis of lymphoid cells expressing the NKp46 cell surface receptor. *Proc. Natl. Acad. Sci. U.S.A.* **108**, 18324–18329 (2011).

45. G. H. Ran, Y. Q. Lin, L. Tian, T. Zhang, D. M. Yan, J. H. Yu, Y. C. Deng, Natural killer cell homing and trafficking in tissues and tumors: From biology to application. *Signal Transduct. Target. Ther.* **7**, 205 (2022).

46. Y. M. Morillon, F. Manzoor, B. Wang, R. Tisch, Isolation and transplantation of different aged murine thymic grafts. *J. Vis. Exp.* e52709 (2015).

47. W. Liao, J. X. Lin, L. Wang, P. Li, W. J. Leonard, Modulation of cytokine receptors by IL-2 broadly regulates differentiation into helper T cell lineages. *Nat. Immunol.* **12**, 551–559 (2011).

48. T. Yoshimoto, K. Takeda, T. Tanaka, K. Ohkusu, S. Kashiwamura, H. Okamura, S. Akira, K. Nakanishi, IL-12 up-regulates IL-18 receptor expression on T cells, Th1 cells, and B cells: Synergism with IL-18 for IFN-γ production. *J. Immunol.* **161**, 3400–3407 (1998).

49. Y. Zhao, P. Liu, Z. Xin, C. Shi, Y. Bai, X. Sun, Y. Zhao, X. Wang, L. Liu, X. Zhao, Z. Chen, H. Zhang, Biological characteristics of severe combined immunodeficient mice produced by CRISPR/Cas9-mediated *Rag2* and *IL2rg* mutation. *Front. Genet.* **10**, 401 (2019).

50. A. C. F. Ferreira, A. C. H. Szeto, M. W. D. Heycock, P. A. Clark, J. A. Walker, A. Crisp, J. L. Barlow, S. Kitching, A. Lim, M. Gogoi, R. Berks, M. Daly, H. E. Jolin, A. N. J. McKenzie, RORα is a critical checkpoint for T cell and ILC2 commitment in the embryonic thymus. *Nat. Immunol.* **22**, 166–178 (2021).

51. L. Qian, S. Bajana, C. Georgescu, V. Peng, H. C. Wang, I. Adrianto, M. Colonna, J. Alberola-Ila, J. D. Wren, X. H. Sun, Suppression of ILC2 differentiation from committed T cell precursors by E protein transcription factors. *J. Exp. Med.* **216**, 884 (2019), 899.

52. T. M. Bigley, L. Yang, L. I. Kang, J. B. Saenz, F. Victorino, W. M. Yokoyama, Disruption of thymic central tolerance by infection with murine roseolovirus induces autoimmune gastritis. *J. Exp. Med.* **219**, e20211403 (2022).

53. P. Tougaard, L. O. L. O. Martinsen, L. F. L. F. Zachariassen, L. Krych, D. S. D. S. Nielsen, T. B. T. B. Buus, A. E. A. E. Pedersen, A. K. A. K. Hansen, S. Skov, C. H. F. C. H. F. Hansen, TL1A aggravates cytokine-induced acute gut inflammation and potentiates infiltration of intraepithelial natural killer cells in mice. *Inflamm. Bowel Dis.* **25**, 510–523 (2019).

54. Y. Kamimura, L. L. Lanier, Rapid and sequential quantitation of salivary gland-associated mouse cytomegalovirus in oral lavage. *J. Virol. Methods* **205**, 53–56 (2014).

55. W. Li, R. N. Germain, M. Y. Gerner, High-dimensional cell-level analysis of tissues with Ce3D multiplex volume imaging. *Nat. Protoc.* **14**, 1708–1733 (2019).

56. Y. Hao, S. Hao, E. Andersen-Nissen, W. M. Mauck, S. Zheng, A. Butler, M. J. Lee, A. J. Wilk, C. Darby, M. Zager, P. Hoffman, M. Stoeckius, E. Papalexi, E. P. Mimitou, J. Jain, A. Srivastava, T. Stuart, L. M. Fleming, B. Yeung, A. J. Rogers, J. M. McElrath, C. A. Blish, R. Gottardo, P. Smibert, R. Satija, Integrated analysis of multimodal single-cell data. *Cell* **184**, 3573–3587.e29 (2021).

57. I. Korsunsky, N. Millard, J. Fan, K. Slowikowsk, F. Zhang, K. Wei, Y. Baglaenko, M. Brenner, P. R. Loh, S. Raychaudhuri, Fast, sensitive and accurate integration of single-cell data with Harmony. *Nat. Methods* **16**, 1289–1296 (2019).